Multi-Disciplinary Design and Performance Assessment of Effective, Agile NATO Air Vehicles

Carsten M. Liersch[1]
DLR – German Aerospace Center, Braunschweig, Germany

Russell M. Cummings[2]
United States Air Force Academy, Colorado Springs, USA

Andreas Schütte[3], Jan Vormweg[4]
DLR – German Aerospace Center, Braunschweig, Germany

Ryan G. Maye[5] and Tiger L. Jeans[6]
University of New Brunswick, Fredericton, Canada

This article belongs to a series of publications about the activities performed within the NATO STO Research Task Group AVT-251 on "Multi-Disciplinary design and performance assessment of effective, agile NATO Air Vehicles". The article concentrates on the development and investigation of the MULDICON UCAV configuration, as well as on the organization and assessment of the AVT-251 task group itself. After a brief introduction to the preceding task groups and the research questions that lead to AVT-251, the selection of design requirements is discussed and the chosen way for developing MULDICON out of its predecessor, the SACCON concept, is sketched. A special focus is placed on the various aerodynamic investigations with the aim to control the vortex flow topology at medium to high angles of attack. Thereafter, the overall aircraft design work on the re-designed outer shape is presented and the resulting MULDICON configuration is investigated and assessed. Finally, a concluding summary of the MULDICON concept and the AVT-251 task group is presented.

Nomenclature

A, B, C	Locations of airfoil sections
A_{ref}	Reference area [m²]
C_D	Drag coefficient [-]
C_L	Lift coefficient [-]
C_m, C_M	Pitching moment coefficient [-]
C_T	Thrust coefficient [-]
I_{xx}, I_{yy}, I_{zz}	Mass moments of inertia around *X*, *Y*, *Z* [kgm²]
R	Leading edge curvature radius [mm]
X, Y, Z	Coordinates [m]
α	Angle of Attack [°]
ε_{LE}	Twist angle (around leading edge) [°]
ε_{TE}	Twist angle (around trailing edge) [°]
φ_{LE}	Leading edge sweep angle [°]
φ_{TE}	Trailing edge sweep angle [°]
c_{ref}	Reference length (MAC) [m]
deg	Degree of arc (also written as °)
kn	Knots (nautical miles per hour)
n_z	Vertical load factor [-]
r	Relative leading edge curvature radius [mm/m]
s	Halfspan [m]
y^+	Non-dimensional value to assess resolution of boundary-layer wall [-]

[1] Research Scientist, Institute of Aerodynamics and Flow Technology, Lilienthalplatz 7, 38108 Braunschweig, Germany, Carsten.Liersch@dlr.de
[2] Director, Hypersonic Vehicle Simulation Institute, USAFA, Colorado Springs, CO, 80840, USA, Russ.Cummings@usafa.edu
[3] Research Scientist, Institute of Aerodynamics and Flow Technology, Lilienthalplatz 7, 38108 Braunschweig, Germany, Andreas.Schuette@dlr.de
[4] Diploma Student, Institute of Aerodynamics and Flow Technology, Lilienthalplatz 7, 38108 Braunschweig, Germany
[5] Master Student, University of New Brunswick, Fredericton, E3B 5A3, NB, Canada
[6] Associate Professor, Department of Mechanical Engineering, University of New Brunswick, Fredericton, E3B 5A3, NB, Canada, tjeans@unb.ca

1 Introduction

The ability to accurately predict both static and dynamic stability characteristics of air vehicles using CFD[7] methods could revolutionize the air vehicle design process, especially for military air vehicles [1]. A validated CFD capability would significantly reduce the number of ground tests required to verify vehicle concepts and, in general, could eliminate costly vehicle 'repair' campaigns required to fix performance anomalies that were not adequately predicted prior to full-scale vehicle development [2-5]. This article outlines the extended integrated experimental and numerical approach performed within the NATO[8] STO[9] Research Task Group AVT[10]-251 on "Multi-Disciplinary design and performance assessment of effective, agile NATO Air Vehicles" and its predecessor groups. While the focus of the previous groups was placed on the assessment and validation of the CFD capabilities to predict complex vortical flows accurately, AVT-251 was dedicated to the application of CFD in the early phase of aircraft design.

1.1 Background

In order to evaluate and improve the prediction of S&C[11] characteristics of highly swept wings at medium to high angles of attack, a number of NATO RTO[12] and STO task groups have been formed in AVT during the past decades. AVT-080 focused on determining the ability of CFD to predict vortical flow structures on delta wings [6]. In AVT-113 [7, 8] the focus was on experimental and numerical investigations on delta wing configurations with various leading edges from sharp to different round radii. AVT-113 started from given fundamental wind tunnel data by NASA followed by several pre-test CFD results which supported the wind tunnel investigations with advanced experimental methods.

1.2 AVT-161

Following the abovementioned task groups, the NATO RTO AVT-161 Task Group was established as a next step to determine the ability of computational methods to accurately predict both static and dynamic stability of air and sea vehicles. Whereas the group concentrated on the air vehicle application, the overall approach was to identify major synergy in terms of physical modeling, fluid structures, or transition effects. The Task Group joined three major avenues of interest: the experimental part to provide highly accurate static and dynamic validation data, the CFD community trying to predict the steady state and dynamic behavior of the target configurations, and the S&C group which was analyzing the experimental and numerical data. The objective of the group was to provide best practice procedures to predict the static and dynamic behavior especially for configurations with vortex-dominated flow fields where non-linear effects have a significant impact. These non-linear regimes are the areas where typical linear S&C methods fail, or where wind tunnel data are only available for non-full-scale flight flow regimes. Currently these deficiencies can only be addressed through costly flight testing. Because of this the main focus was the prediction with CFD methods rather than enhancing existing S&C system identification methods.

In an attempt to insure that the computational requirements for the experimental data were included in the planning as the Task Group progressed, the CFD participants were asked early in the program to identify a "wish list" of experimental results. The over-arching theme of the responses can best be summarized as: *understand the developing flow structures*. In other words, the CFD community not only wanted to know the gross aerodynamics of the vehicle, but also the causes of any interesting/unusual flow phenomena. This request was nearly unanimous and quite strongly stated by the CFD members, and the experimental researchers kept the requests in mind as they designed the wind tunnel tests.

Since the overall goal of AVT-161 was to determine the ability of modern CFD tools to adequately predict static and dynamic S&C parameters for modern aircraft, two candidate configurations were chosen: the X-31 and a generic UCAV[13] configuration called SACCON[14]. The latter one was designed especially for the AVT-161 task group, with the aim to exhibit a highly complex aerodynamic behavior, serving as a challenge for numerical flow prediction using CFD methods. Both AVT-161 Task Group target configurations possess a delta wing planform with medium sweep leading edges (between 45° and 57° sweep angle), and with leading edge nose radii varying from sharp to medium and large roundness. The approach was to provide most (if not all) flow features common to typical UCAV and fighter aircraft configurations, and to investigate the aerodynamic challenges which have to be captured by computational methods. An overview of the AVT-161 Task Group is provided by Cummings et al. [9, 10].

---

[7] **C**omputational **F**luid **D**ynamics
[8] **N**orth **A**tlantic **T**reaty **O**rganization
[9] NATO **S**cience and **T**echnology **O**rganization
[10] **A**pplied **V**ehicle **T**echnology Panel
[11] **S**tability **&** **C**ontrol
[12] NATO **R**esearch and **T**echnology **O**rganization
[13] **U**nmanned **C**ombat **A**erial **V**ehicle
[14] **S**tability **A**nd **C**ontrol **CON**figuration

1.3 AVT-183

During AVT-161, the SACCON configuration exhibited a number of very uncommon flow features, related to its variable leading edge roundness along the wingspan. As a consequence, the AVT-183 Task Group on "Reliable Prediction of Separated Flow Onset and Progression for Air and Sea Vehicles" was founded to gain a deeper understanding of the separation onset and progression of the flow at round leading edges. Experimental and numerical results of AVT-183 are, beside others, published by Hövelmann and Breitsamter [11], as well as by Frink [12]. All of these investigations resulted in improved understanding of the flow physics and new best practice methods for computational simulation of vortical flows.

1.4 AVT-201

The NATO STO AVT-201 Task Group was established as an extension to the AVT-161 Task Group. While the purpose of AVT-161 was to determine the ability of computational methods to accurately predict both static and dynamic stability of air and sea vehicles, AVT-201 took on the additional tasks of including control surface deflections in the aerodynamic evaluation, as well as to investigate ways to create full flight simulations using CFD. Again, the group concentrated on the air vehicle application, but the overall approach still was to identify major synergy in terms of physical modeling, fluid structures, or transition effects [13, 14].

The topics covered by AVT-201 included the following:

- Perform additional in-depth correlation studies
    - Evaluate the ability of CFD to accurately predict S&C for dynamic maneuvers using experimental data obtained by AVT-161
    - Use the detailed flow field measurements (such as PIV data) obtained by AVT-161 to enhance understanding of discrepancies between predicted and experimental dynamic derivatives
    - Further analyses of AVT-161 data for cases with flow asymmetry and highly unsteady flow to extend understanding of vehicle dynamics (air activity)
    - Perform additional wind and/or water tunnel/channel testing to extend the dynamic data set to include multiple frequency and amplitude maneuvers to improve the determination of realistic dynamic derivatives
    - Obtain, where possible, full-scale test data for a maneuvering vehicle that can be used for validation of the methods and capabilities that are developed
- Investigate control surface effects on dynamic S&C
    - Design, build, and test modified SACCON wind tunnel model with trailing-edge control surfaces (static deflections)
    - Evaluate the ability to predict control effectiveness, stability characteristics, and other flight mechanic characteristics of the configuration with controls deflected
- Investigate techniques for creating flight simulation models from CFD predictions
    - Build S&C data bases from experimental and CFD predictions to compare impact on flight simulation accuracy
    - Determine level of accuracy and sensitivity of flight simulation using CFD when compared with the experimental data model
    - Explore range of strategies for creating CFD-derived simulation models across the flight envelope (such as reduced-order modeling or combined low-fidelity/high-fidelity approaches)
- International collaboration
    - The concept of a virtual laboratory, as pioneered by AVT-113, and used to great effect in AVT-161, shall be employed by AVT-201 in order to make the data being measured and computed available to the participants on a timely basis

There were 16 different organizations making contributions from 5 different NATO nations, as well as Sweden and Australia. A wide variety of contributions were included, such as wind tunnel model development, wind tunnel testing, CFD predictions, engineering method analysis, and development of S&C models of various types. This represents a wide variety of participation that made the AVT-201 a highly productive and successful task group.

1.5 AVT-251

After completing AVT-161 and AVT-201, a comprehensive knowledgebase about the flow physics of SACCON-like configurations had been gathered. These are experimental (see among others [15, 16]) and numerical (see among others [17-20]) data at a Mach number range from 0.12 to 0.9. This data includes symmetrical and asymmetrical cases

for steady and unsteady flow conditions. Furthermore, a large amount of expertise was available, covering the knowledge of how to simulate such sort of configuration using CFD methods and the reliability of the corresponding results. The next logical step was to use all this knowledge and experience to re-design the SACCON configuration into a more realistic aircraft concept.

1.5.1 Objectives

As mentioned above, the initial design of the SACCON outer shape was developed in 2007 and 2008 by partners from AVT-161 in order to have a common, generic UCAV configuration for research purposes. One of the ideas behind SACCON was to have a geometry which could exactly be reproduced in a wind tunnel model as well as in a CFD mesh. The conceptual design task performed in AVT-201 was to design an internal layout into the original SACCON outer shape. This means, that it was only permitted to scale the entire SACCON geometry to a suitable size and to cut out parts for integrating components like control surfaces or engine inlets and nozzles. This work resulted in a 25% increase compared to the initially planned SACCON size, in order to fit the required fuel and all the main components into the aircraft [13]. However, the final configuration still exposed the complex flow phenomena which are very interesting to study, but which are highly undesirable for a realistic aircraft concept.

AVT-251 was established in order to accept that challenge: Within a three-year-period of time, a multi-disciplinary re-design of the SACCON configuration towards a realistic aircraft concept named MULDICON[15] should be performed. Therefore, the group would have to deal with non-linear aerodynamic flow physics, control device strategies for the medium to high angle of attack flight regimes and vortical flow fields, as well as with the design aspects regarding propulsion systems and signature constraints – everything relying purely on CFD and other numerical methods. From the beginning on it was clear that a comprehensive investigation covering all relevant aspects of the design would be beyond the scope of the group. Instead, it was tried to focus the available resources and partners to some of the most critical aspects and link everything together using conceptual aircraft design methods [21].

Specifically, the objectives of AVT-251 were:

- Re-design an effective and agile UAV
- Highest possible contribution of multiple disciplines
- Development of a flight mechanics model by use of CFD, ROM[16] etc. (no wind tunnel testing)
- Assess the performance at specific points of a defined flight envelope
- Development of control laws for specific points of the defined flight envelope
- Development of a design process

In addition, AVT-251 was to answer the following questions:

- How do the tools contribute to the design process?
- How do the tools accelerate the design process?
- How do we arrange the tools in sequence or in parallel during the design process?
- To what degree can CFD methods provide sufficient data for a flight mechanics model?
- To what degree can other disciplines provide inputs to the process?

It was important to remember that AVT-251 was not designing a competitive configuration, rather about finding ways to improve the design process while designing a realistic vehicle. The basic approach for AVT-251 was to:

- Use the SACCON as a starting planform
- Use the existing experiments from AVT-161 and AVT-201 for validation
- Use CFD experience to provide the aerodynamic data set (for parts of the mission or mission points)
- Integrate disciplines in parallel or in sequence depending on the group contributions:
  - Aerodynamics
  - Control device strategy
  - Propulsion system: intake, engine, nozzle
  - Signature requirements
  - Structure and/or Aeroelasticity, etc.
  - Formulate a design strategy

[15] **MUL**ti-**DI**sciplinary **CON**figuration
[16] **R**educed **O**rder **M**odel

1.5.2 Approach

Before the group officially started, some of the partners contributed to a preparatory team, called “Design Specification Group” (DSG). The aim of the team was to prepare a set of requirements, serving as a basis for the planned SACCON re-design work. Out of this team the “Design Specification and Assessment Group” (DSAG) was then formed later on. During AVT-251, the DSAG was–on the one hand–responsible for extending and updating the design requirements document. On the other hand, the DSAG had to perform overall design assessment studies using conceptual aircraft design methods.

Recent low observable military flight vehicles from different nations can be assumed to be flying within the low angle of attack range. The aerodynamic behavior is typically linear and critical aerodynamic states are usually avoided. The requirements of some recent designs might demand for being able to fly at higher angles of attack and having more agility compared with the earlier designs. These advanced requirements lead to the necessity to be able to handle the resulting non-linear aerodynamic effects, vortical flow aerodynamics and to be able to adequately predict totally different S&C behavior, as it appears for configurations like SACCON. Thus, one of the main activities in AVT-251 was the re-design of the outer shape of SACCON, in order to improve its aerodynamic performance and remove the undesirable characteristics which were revealed in the AVT predecessor groups. This task was given to the second (and biggest) design team within AVT-251, the “Aerodynamic Shaping Group (ASG).

The third design team of AVT-251 was the “Control Concept Group” (CCG). Its task was two-fold: On the one hand, the team had to investigate and specify a suitable set of control surfaces, sufficient to achieve the demanded performance requirements; on the other hand, they had to investigate the performance characteristics of the overall aircraft as it came out of the overall aircraft design process. Especially the second task could only be performed in a very limited way, due to a lack of contributing partners in that field.

For such a highly integrated aircraft configuration with the general demand for low observability, the integration of the engine (including intake and nozzle) is another crucial aspect. While the design of the engine itself was not a direct part of AVT-251, but kindly provided by DLR, the integration of that engine into the aircraft was investigated by the “Engine Integration Group” (EIG).

The last design team in AVT-251 was dedicated to the investigation of structural and aeroelastic aspects. The “Structural Concept Group” (SCG) provided a basic concept for the structural topology and a corresponding primary structure mass to the overall aircraft design process. Furthermore, static and dynamic aeroelastic effects were investigated for the new configuration.

Besides the task to provide a general introduction and an overview of the activities performed within AVT-251, this article focuses on three major topics. The first part (see Chapter 2) is dedicated to the selection and specification of the design requirements for the new aircraft concept, which was performed by the DSAG. The second topic (see Chapter 3) presents some basic aerodynamic studies which were performed by the ASG in an attempt to control the vortex development with increasing angle of attack. The third part of this article (see Chapter 4) provides an overview of the overall aircraft design activities of the DSAG and the resulting aircraft configuration. A final section (see Chapter 5) summarizes the work of AVT-251 with respect to the design task and the task group itself.

2 Design Task

2.1 Background

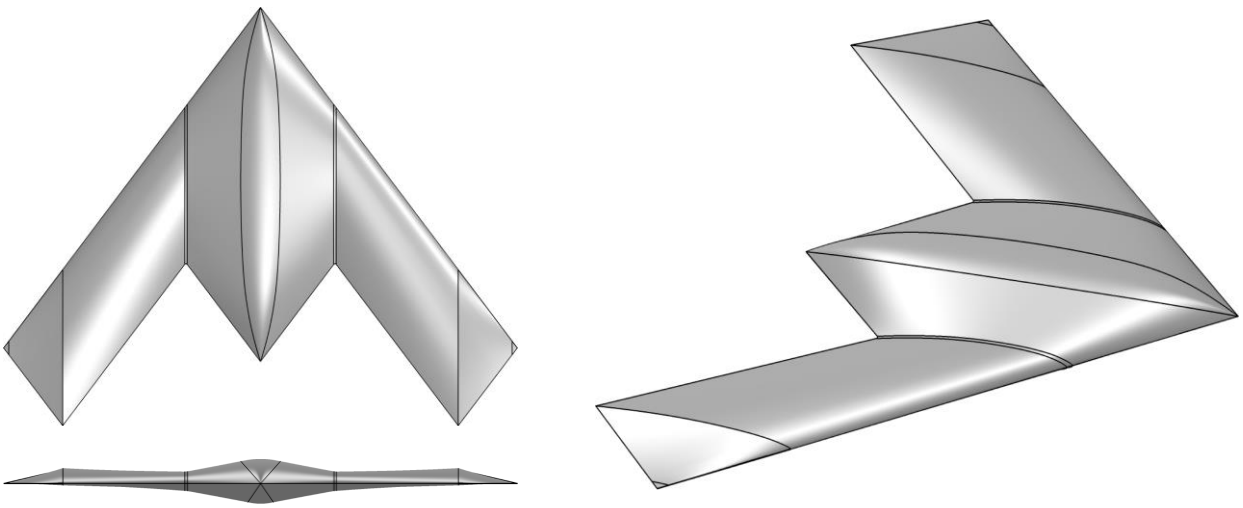

Figure 1: Outer shape of the SACCON configuration

The starting point for the aircraft design work within AVT-251 was the abovementioned SACCON configuration, a tailless, lambda-shaped flying wing UCAV concept, characterized by a 53° swept wing with parallel edges for low radar signature purposes (see Figure 1). SACCON is a common research concept which was initially defined by the NATO STO Task Group AVT-161 on "Assessment of Stability and Control Prediction Methods for NATO Air & Sea Vehicles" as a benchmark for CFD methods and wind tunnel experiments [9, 10]. Due to its leading edge shape defining radius, varying continuously from sharp to round and back to sharp, it exposes complex, vortex-dominated flow structures which are highly challenging to predict.

The SACCON concept, as it was specified in AVT-161, was a pure outer shape. Within the successor Task Group AVT-201 on "Extended Assessment of Stability and Control Prediction Methods for NATO Air Vehicles", an attempt was made to turn the SACCON shape into a reasonable aircraft concept. Therefore, a set of design requirements were defined for SACCON, including a design mission to be flown, a payload to be carried, and some further parameters like fuel reserve and stability margin. As it was decided that the outer shape of SACCON should be preserved in order to stay consistent with existing CFD and wind tunnel data, the aircraft had to be scaled until the internal volume and dimensions became sufficiently large. Convergence was finally reached at a wingspan of 15.375 m and a MTOM[17] of approximately 15 metric tons. The whole concept is sketched in Figure 2.

During these studies it turned out that an internal arrangement with a single, central engine (shown in green) and two payload/weapon bays aside (shown in yellow) offers the best opportunity for efficient propulsion with a low SFC[18]. Even though this concept limits the possible size of a single, large payload, it is an essential prerequisite for reaching the specified mission range of 3 000 km plus an additional fuel reserve of 45 min. In order to limit the CG[19] movement due to fuel consumption, a concept with two fuel tanks (shown in red) on each side having a common CG within the specified CG range was chosen. The complete design process carried out during AVT-201 is described in detail in Refs. [13, 14, 22].

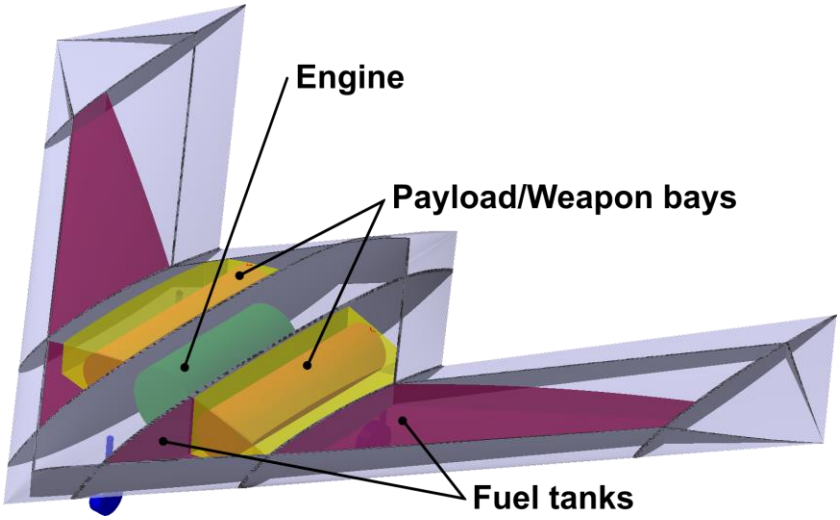

Figure 2: SACCON UCAV concept

Even though a basic mission capability could be reached for the SACCON concept, several unsatisfactory aspects that demanded significant changes in the outer shape were identified. In AVT-201's successor group, AVT-251, the main focus was to re-design the outer shape using high-fidelity aerodynamic methods (proven for this kind of flow topology during the SACCON related AVT Task Groups) in order to overcome the identified shortcomings of the concept. The subsequent chapters of this article describe the identification and specification of design requirements, as well as the design process and the resulting MULDICON concept.

2.2 MULDICON Design Requirements

The rationale behind the development of the MULDICON concept is to overcome the known deficiencies of the SACCON concept and to evolve it into controllable and agile UCAV configuration which is consistent from a conceptual aircraft design point of view. In order to stay as close to the SACCON concept as possible, it was agreed that most of the requirements from SACCON should remain the same and that the changes of the geometry should be limited to a minimum. The following sections discuss the various design requirements in detail.

2.2.1 Design Mission

The design mission for MULDICON was taken from SACCON without any change. Altitude and Mach number are sketched over distance to the starting point (from left to right and back to the left) in Figure 3.

[17] **M**aximum **T**ake**O**ff **M**ass
[18] **S**pecific **F**uel **C**onsumption
[19] **C**enter of **G**ravity

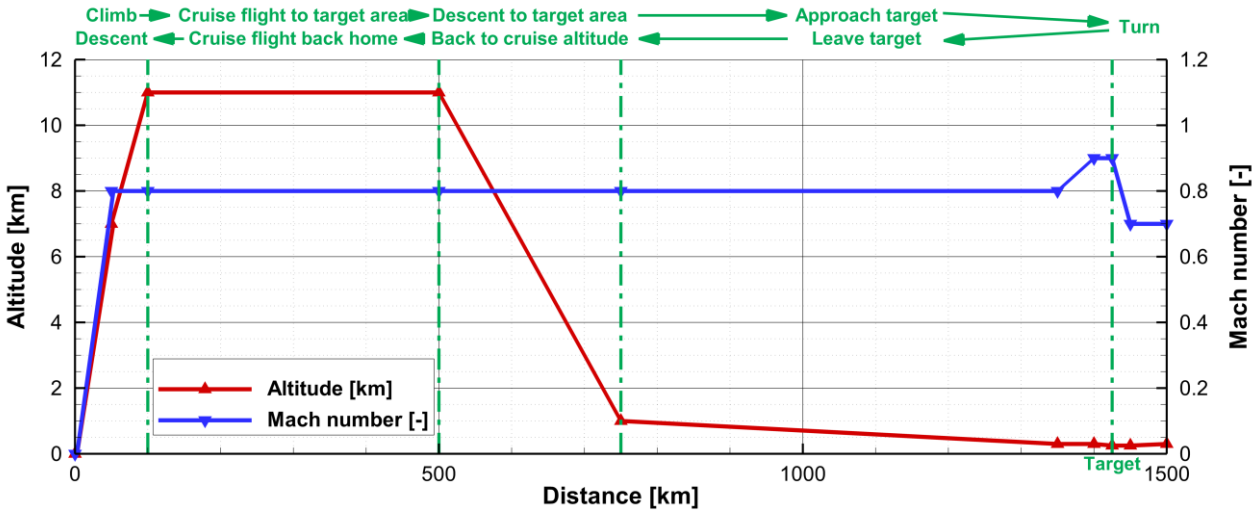

Figure 3: MULDICON design mission

It is a rather classical long range transport mission with a radius of 1 500 km and no aerial refueling, closely related to "Bomber – low-level penetration" from the United States Military Standard MIL-STD-3013 [23]. It consists of two main parts, a high altitude cruise segment, followed by a low altitude dash approaching the target. After passing the target, it continues with a turn and returns to base over the same flight profile. Nearly all the mission is flown with a Mach number of 0.8 – except for the initial climb / final descent and the turn after passing the target. During the last 75 km before reaching the target area, the speed could be further increased up to a Mach number of 0.9 or below – depending on the available thrust of the engine (and maybe other limitations like permitted dynamic pressure). However, this acceleration is just an option to exploit existing reserves of the aircraft and not a design requirement itself. The high level cruise flight segment is performed at an altitude of 11 km, the low level dash when approaching and leaving the target is started at an altitude of 1 000 m, descending to 300 m and climbing back to 1 000 m on the way back. An additional fuel reserve of approximately 45 min of flight time is desired.

In addition to the basic mission, as it was specified for SACCON, maneuver agility and other requirements for each section of the mission were defined, mostly based on the United States Military Standard MIL-STD-1797A[20] [24].

2.2.2 Payload

As for SACCON, it was decided to also use the configuration layout one central engine with a payload/weapon bay on either side for MULDICON. In order to determine the required size of the bays and the maximum payload mass to be carried, a weapon systems study was performed. With respect to different possible weapons, a payload/weapon bay length of 4.2 m and a width of 1.0 m was chosen. The height of the bay depends on the outer shape and the structural concept of the aircraft. The maximum payload mass for each weapon bay has been agreed to be 1 250 kg. The payload/weapon bay shall be located within the permitted CG range in order to minimize CG movement due to weapon release.

2.2.3 Agility and Control Concept

With respect to the demand of evolving SACCON into a controllable, agile UCAV, there are several new requirements coming from the field of S&C. First of all, SACCON is lacking a reasonable control concept. It is equipped with two trailing edge control surfaces on each side of the wing for roll and pitch control, as can be seen in Figure 4. During the investigations of AVT-201 it turned out that–due to the high trailing edge sweep of the wing–these control surfaces exhibit very poor performance. Such a performance assessment can be done, e.g. by comparing data from high-fidelity RANS[21] CFD or wind tunnel tests to results from low-fidelity CFD based on the linearized potential flow equations. As the latter methods always assume attached flow, their results can be seen as an assumption for control surfaces with an optimal performance–at least as long as vortex-induced additional lift effects can be neglected. Such comparisons are performed in [22, 25] and they show strong discrepancies between low- and high fidelity results. The overall roll performance of SACCON based on low-fidelity aerodynamics, as well as on experimental data from wind tunnel tests is discussed by Ehlers et al. [26] (Fig. 17, p. 658). In that article, the roll performance based on the low-fidelity aerodynamics dataset is shown to be sufficient for this type of aircraft, but when applying the aerodynamic results from wind tunnel tests instead, the roll performance becomes very poor. An impression of the complex flow topology of the SACCON configuration with deflected control surfaces which leads to these effects is provided in Figure 5.

---

[20] Even though MULDICON is not a piloted aircraft, many of the requirements form this standard seem to be appropriate here, as well.
[21] **R**eynolds-**A**veraged **N**avier-**S**tokes Equations

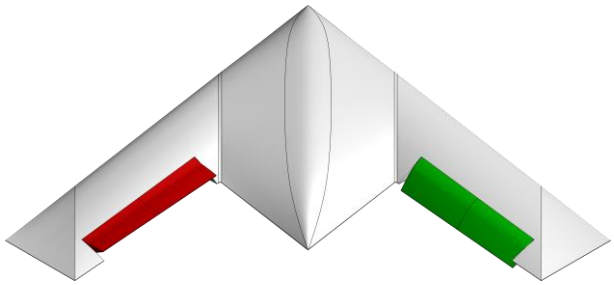

Figure 4: SACCON control surfaces (taken from [16])

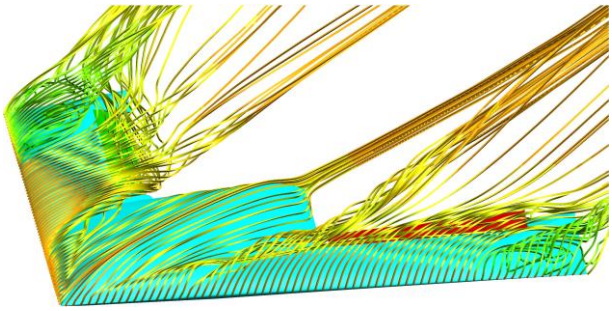

Figure 5: Impression of flow around SACCON with deflected control surfaces (taken from [27])

Considering yaw control, several different flap and spoiler concepts were studied for SACCON [28], but none of these performed well. Again, the main reason for the limited control effectiveness seems to have its roots in the high trailing edge sweep of the wing. As a consequence of these control problems, it was agreed in AVT-251 that the trailing edge sweep of MULDICON should be reduced from 53° (as it was for SACCON) to 30°. Even though this certainly adds additional peaks to its radar signature, it was assumed that the performance of the trailing edge devices would be enhanced and that the modified flow would also enable an appropriate yaw control concept. In order to define agility requirements for MULDICON, five dedicated design points covering various flight conditions were selected and specified. Even though agility requirements for each segment of the design mission were already defined (as described in section 2.2.1), with respect to the resources available in AVT-251 it was agreed to focus on these five points only. Table 1 lists the flight conditions for the design points and the corresponding requirements for MULDICON.

		Cruise	**Takeoff**	**Combat Low Altitude**	**Approach**	**Combat High Altitude**
Flight conditions	Altitude	11 000 m	0 m	0 m	0 m	11 000 m
	Mach number	0.8	0.2	0.8	0.4	0.8
	Velocity	236 m/s	68 m/s	272 m/s	136 m/s	236 m/s
	Mass	15 000 kg	15 000 kg	13 000 kg	13 000 kg	13 000 kg
	Vertical load factor	1.0	1.5	4.5	2.5	4.5
	Approximated turn radius	–	422 m	1 722 m	824 m	1 314 m
	Assumed lift-to-drag ratio	20.0	7.0	20.0	16.1	7.0
Design requirements	Roll performance	90° / 1.7 s	30° / 1.1 s	130° / 1.0 s	90° / 1.7s	130° / 1.0 s
	Pitch rate	20°/s	20°/s	20°/s	20°/s	20°/s
	Yaw rate	10-15°/s	10-15°/s	10-15°/s	10-15°/s	10-15°/s
	Permitted crosswind	–	30 kn (15.43 m/s)	–	–	–
	Lift coefficient	0.184	1	0.162	0.361	0.717
	Maximum lift coefficient	0.284	1.1	0.262	0.461	0.817
	(Max. lift coefficient SACCON) (corresponding angle of attack)	*(≈0.65) (≈12–14°)*	*(≈0.90) (≈20–21°)*	*(≈0.65) (≈12–14°)*	*(-)*	*(≈0.65) (≈12–14°)*
	Assumed drag coefficient (for Engine design)	0.0092	0.1429	0.0081	0.0224	–
	Sustained turn thrust demand (for Engine design)	–	32.15 kN	29.23 kN	20.13 kN	–

Table 1: MULDICON design points

Each design point consists of altitude, velocity, mass, and vertical load factor. There are two mass cases: 15 000 kg (Design MTOM) and 13 000 kg (Design MTOM, after use of 1/3 of maximum fuel). The vertical load factors can be seen as pull-up or turn requirements. In case of performing a sustained turn[22] with the defined load factor, an approximation for the corresponding turn radius is provided, as well. The last entry under "Flight conditions" contains an assumption for the lift-to-drag ratio in that flight point (including the load factor), guessed by the DSAG. The "Design requirements" part of the table contains first the specified roll, pitch and yaw requirements. These are either given for a steady rotation rate in degrees per second, or as a performance requirement to reach a certain angle within a specified time, starting from steady, horizontal flight. Aside from the specified yaw rate, there are two further main aspects which are crucial for sizing the yaw control concept: the ability to apply yawing moments rapidly, in order to compensate the expected directional instability of MULDICON and the so-called "de-crab" maneuver for landing under maximum permitted crosswind conditions. The requirement on permitted crosswind for takeoff and landing is again taken from MIL-STD-1797A [24] and provided in the next line of the table. The lift coefficients in the following line are necessary to fly in that point and with the given load factor; the maximum lift coefficients (which are the lift coefficients, increased by a safety margin of 0.1) are the requirements for the design work of the Aerodynamic Shaping Group: MULDICON shall be able to reach that maximum lift coefficient under the specified flight conditions. In order to provide an idea of the required changes compared to SACCON, the subsequent line gives an assumption of the maximum lift coefficients of SACCON for the same cases. Using lift coefficient and lift-to-drag ratio from above, the assumed drag coefficient and the required thrust for a sustained turn are calculated and placed in the last two lines. These are essential requirements for the engine design work. It has to be mentioned that for the "Combat High Altitude" case a sustained turn requirement was not specified. Under such flight conditions, a sustained turn with a load factor of 4.5 would not be reasonable with respect to the selected engine concept [23] (see section 2.2.5).

2.2.4 CG Range and Pitching Moment Characteristic

From SACCON it is already known that development, movement and interaction of vortices with increasing angle of attack severely influence the pitching moment characteristics. These effects were investigated in detail by Schütte et al. [29] and lead to a diagram which is shown in Figure 6. Looking at the pitching moment curve of SACCON, it becomes apparent that such a nonlinear characteristic is not acceptable for a combat aircraft operating at angles of attack up to 20° or even beyond. Thus, one major design task for the Aerodynamic Shaping Group was to modify the outer shape in such a way that the pitching moment characteristic becomes much smoother.

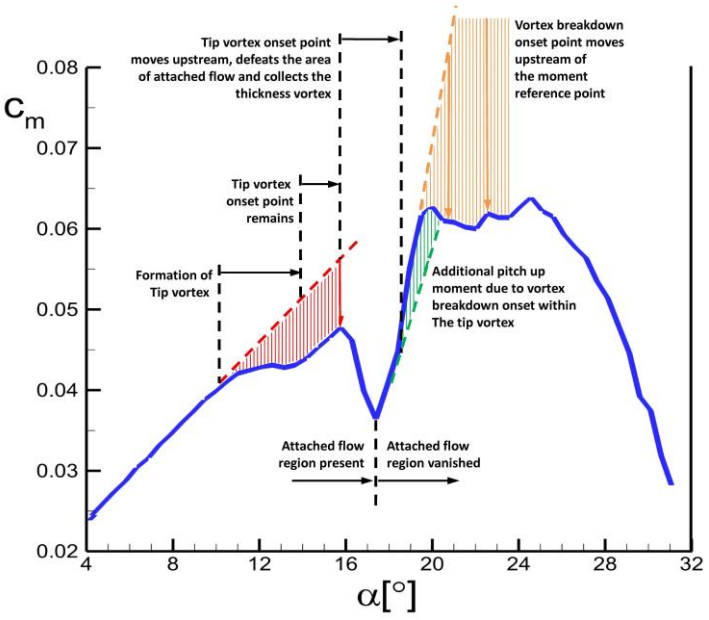

Figure 6: SACCON pitching moment curve (taken from [29])

In order to increase the agility of MULDICON around the pitch axis (compared to SACCON), the permitted CG range was reduced down from 2 – 8% MAC[24] (SACCON) to 0 – 3% MAC (MULDICON) on the stable side of the neutral point[25]. After performing some first computations, the neutral point was approximated to lie 6 m behind the nose of the aircraft. This neutral point is also taken as MRP[26] for the aerodynamic investigations. Together with a MAC length of 6 m (which is taken as reference length for normalizing all three moment coefficients, as well), this leads to a permitted CG range between 5.82 m and 6 m, counted from the nose of the aircraft.

2.2.5 Propulsion

For efficiency reasons, the MULDICON configuration shall be designed with a single, central engine without afterburner (see section 2.1). Based on experience from SACCON, the static dry thrust of the engine shall correspond to

[22] "Sustained turn" means a turn without changing altitude or speed.
[23] For that combination of velocity, altitude and load factor, the required thrust would be around 83 kN.
[24] **M**ean **A**erodynamic **C**hord
[25] Due to the vortex-dominated flow topology, there is not one single neutral point. However, with respect to the design requirement of smoothing the pitching moment curve, it is still reasonable to assume an average position for it.
[26] **M**oment **R**eference **P**oint

a thrust-to-weight ratio of 0.4; for an estimated MTOM of 15 metric tons, this leads a thrust value of 60 kN. The engine shall be optimized for cruise performance (see design point "Cruise" in Table 1); however, its fan diameter shall not exceed 1 m. On top of these requirements, which are rather similar to those of SACCON, the MULDICON engine needs to deliver sufficient thrust for performing the sustained turn maneuvers that are described above in section 2.2.3.

Parameter	Value
Outer shape	Based on SACCON, ±30° trailing edge sweep
Propulsion	Single turbofan engine without afterburner
Propulsion integration	Internal (due to signature reasons)
Static dry thrust	Thrust-to-weight ratio = 0.4 (≈ 60 kN)
Payload storage	Internal (due to signature reasons)
Payload bay size	Length: 4.2 m, Width: 1.0 m
Payload mass	2 × 1 250 kg
Design range	3 000 km (without aerial refueling)
Fuel reserve	≈ 45 min
Cruise altitude	11 km
Cruise Mach number	0.8 (all altitudes)
Stability margin	0 − 3% MAC (stable)
CG range	5.82 m – 6.00 m

Table 2: Main design parameters of MULDICON

2.2.6 General Aspects

With respect to the amount of time and resources being available for the design of MULDICON, the disciplinary design teams had to work in parallel with a very small number of interdisciplinary iterations between them. Hence, it could happen that the results of the different teams are not fully consistent anymore. It was the task of the Design Specification and Assessment Group to harmonize the parallel work of the disciplines as far as possible and to provide assumptions for parameters that were not available at the time when they were required. Concluding the specification of design requirements for MULDICON, an overview of the main parameters is collected and listed in Table 2.

3 Numerical Investigations

The understanding and prediction of the flow physics of delta wing configurations with round or variable leading edges is still challenging and a key issue for the design process of aircraft configurations with a vortex dominated flow field. Accepting that challenge, the SACCON concept has been investigated experimentally and numerically by several NATO AVT research task groups for more than a decade now (see Chapter 1). As a result of these investigations, a deeper understanding of the separation onset and progression of the flow at round leading edges was gained. The description of the separation mechanism process described by Frink [12] has been systematically extended by Schütte [30] to show how the flow physics develops by changing the leading edge contour and onflow conditions. It was documented at which onflow conditions for a particular leading edge geometry the vortex occurs and how it progresses depending on the angle of attack, leading edge sweep and onflow Mach number. The sensitivity and studies of the flow topology on the aerodynamic behavior lead to design guidelines for configurations with swept wings and round leading edges.

Based on this extended knowledge about flow physics, design guidelines and the use of validated computational methods for such an aircraft shape, several design studies were conducted within the Aerodynamic Shaping Group of AVT-251. A part of these studies, performed by the University of New Brunswick in Canada and the DLR is presented in this chapter. The aim of these specific studies was to provide a solid, vortical flow dependent design based on SACCON, which meets the requirements specified in the previous chapter.

3.1 MULDICON Planform and Design Parameters

The MULDICON shape is based on the SACCON configuration. Both planforms share the same span and leading edge sweep angle of 53º. In order to enhance the effectiveness of trailing edge control devices (which turned out to be rather inefficient for SACCON [16]), the trailing edge sweep was reduced to 30°. The differences in planform, as well as the main geometric properties are shown in Figure 7. With respect to this new shape, the planform area (used as reference area A_{ref}) for MULDICON increases to 77.8 m² (compared to 77.2 m² planform area and 77 m² reference area for SACCON), while the halfspan s stays the same (7.696 m). So, both configurations share an aspect ratio of 3. As reference length (MAC) for the three moment coefficients and for the Reynolds number, the chord length of the inner kink c_{ref} was selected, which is 6 m for MULDICON (compared to 4.79 m for SACCON). All forces and moments are related to the MRP (which is identical the most rearward permitted CG location for MULDICON), located 6 m behind the nose of the aircraft for both configurations. For the design studies presented below, the airfoils used in the definition sections *A*, *B* and *C* are modified in several different ways. Furthermore, the inner part of the configuration is changed in order to integrate a generic intake and nozzle for the engine.

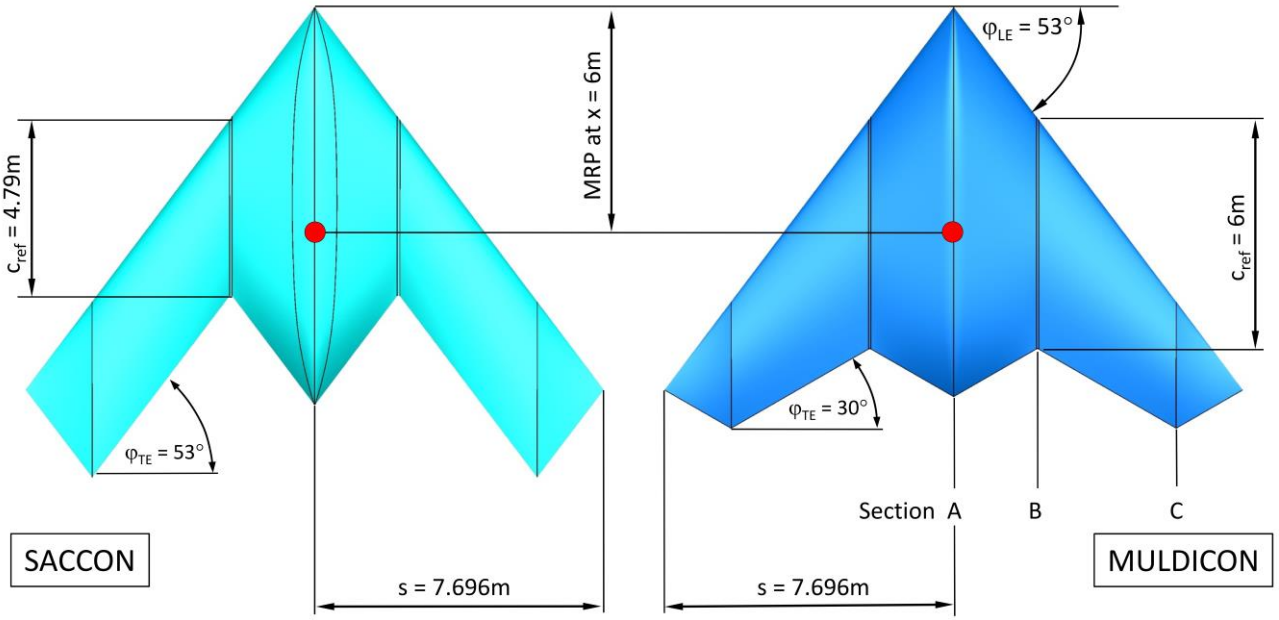

Figure 7: Planform and reference data SACCON and MULDICON

3.2 Numerical Approach

For the aerodynamic design approach two different computational RANS methods have been applied. Both have in common that they use a hybrid computational grid approach, but the DLR TAU-Code is based on a cell-vertex scheme, while the USAFA[27] CFD solver Cobalt uses a cell-centered scheme. In order to make the grid sizes of these different concepts comparable, they are provided in grid points for TAU, while they are given in cells for Cobalt.

3.2.1 DLR Flow Solver TAU

The DLR RANS solver TAU is developed by the DLR Institute of Aerodynamics and Flow Technology [31]. It solves the compressible, three-dimensional, time-accurate Reynolds-Averaged Navier-Stokes equations using a finite volume formulation. The code is based on a hybrid unstructured-grid approach to be able to handle structured and hybrid computational grids, which makes use of the advantages offered by prismatic grid structures used for the resolution of viscous shear layers near walls, and the flexibility in grid generation offered by unstructured grids. By sub-dividing the grid, TAU permits highly parallelized computations on large computer clusters.

The current simulations have been performed using the steady state and unsteady dual time-stepping approach [32]. The dual time stepping approach was used to achieve a steady state results by averaging over a certain time period. The latter was always applied in cases where no steady state solution could be obtained. For the numerical simulations a version of the one equation Spalart-Allmaras turbulence model [33] called “SA-neg” has been applied. The SA-neg version allows particularly negative values of the transport turbulence quantities [34]. This modification should lead to a more efficient solution of the equation without changing the final aerodynamic solution.

The hybrid unstructured grids used for the simulations with TAU have been created with the hybrid grid generator Centaur, developed by CentaurSoft [35]. The grid topology and local grid refinement are based on best practice approaches from previous numerical validation of the DLR RANS method TAU, e.g. published by Schütte et al. in [29]. Figure 8 shows an example of the grid topology. The prismatic layer is colored in yellow. Furthermore, the refinement of the tetrahedral grid in the field can be seen colored in green. This refinement is based on an approximation of the element size compared to vortex size and is done using a field source and increases the grid resolution in the area above the upper wing where the vortices appear. The grid topology and refinement are done in the same way for all computational grids. Figure 9 shows the surface grid refinement at the leading edge. For all hybrid grids the spacing of the first prismatic layer normal to the wall is 0.005 mm, resulting in a typical y^+ value of approximately one. The boundary layer is fully resolved by 30 prismatic layers. Over the entire surface of the configuration the full 30 prismatic layers can be achieved therefore no chopping of the prismatic layer occurs. The overall size of the different computational grids is approximately 21 million grid points for a half model configuration.

[27] **U**nited **S**tates **A**ir **F**orce **A**cademy

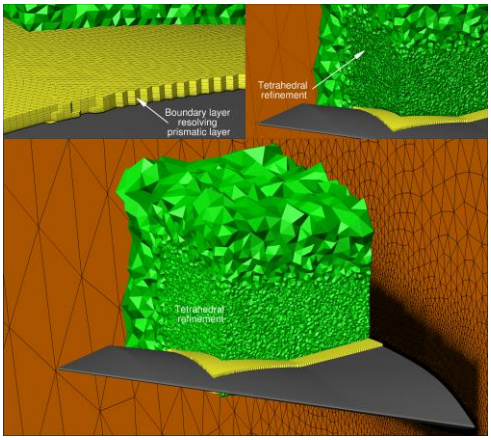

Figure 8: TAU full grid domain

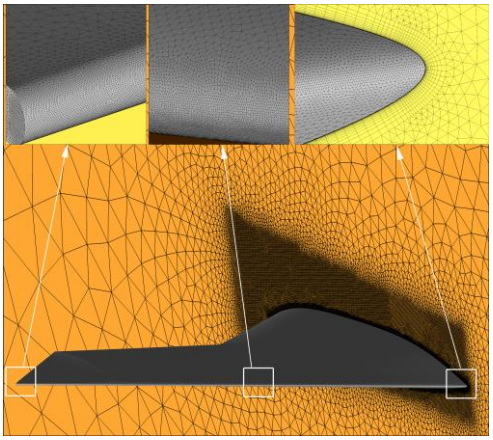

Figure 9: TAU surface grid topology

3.2.2 USAFA Flow Solver Cobalt

The flow solver Cobalt is developed and provided by the US AFRL[28]. It solves the unsteady, three-dimensional, compressible Navier-Stokes equations in an inertial reference frame. The RANS solver Cobalt uses hybrid computational grids which mean arbitrary cell types in two or three dimensions are applied [36]. In Cobalt, the Navier-Stokes equations are discretized on arbitrary grid topologies using a cell-centered finite volume method. A second-order accuracy in space is achieved using the exact Riemann solver of Gottlieb and Groth [37], and a least squares gradient calculations using QR factorization. To accelerate the solution of the discretized system, a point-implicit method using analytic first-order inviscid and viscous Jacobians is used. A Newtonian sub-iteration method is used to improve the time accuracy of the point-implicit method. An approach from Tomaro et al. [38] converted the code from explicit to implicit, enabling CFL[29] numbers as high as 10^6. In Cobalt, the computational grid can be divided into group of cells, or zones, for parallel processing, where high performance and scalability can be achieved even on ten thousands of processors [39].

All Cobalt simulations were run using the SARC[30] turbulence model. The choice of a SARC turbulence model was due to the relative success of this model in previous AVT Task Groups, see Lofthouse et al. [40]. A second order spatial accuracy was chosen, as it allows for gradients within a given cell. Simulations were run with first order temporal accuracy, which is often used for steady-state calculations [41]. The structured grid topology, resolution and size is related to best practice approaches from previous research publications regarding the SACCON geometry within AVT-201 by Kennet et al. [42] and Roy et al. [43]. The structured MULDICON grid is of O-grid style with an initial cell height of 0.012 mm and a growth rate of 1.2 normal to the body for approximately 15 layers. The cell count of the entire half span grid is approximately 29 million. The details of the inner grid and the surface mesh on the MULDICON surface are visible in Figure 10 and Figure 11. The final grid was chosen based on a grid sensitivity study evaluating the lift, drag and pitching moment versus grid size.

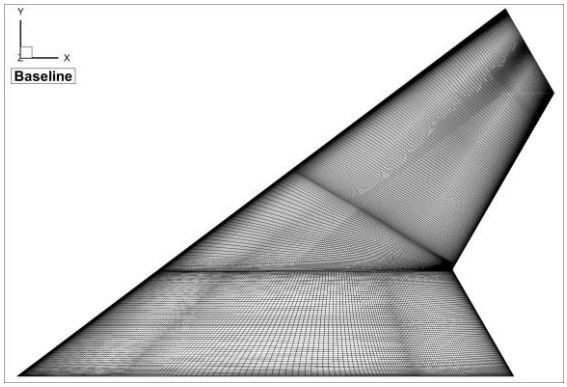

Figure 10: Cobalt surface grid topology

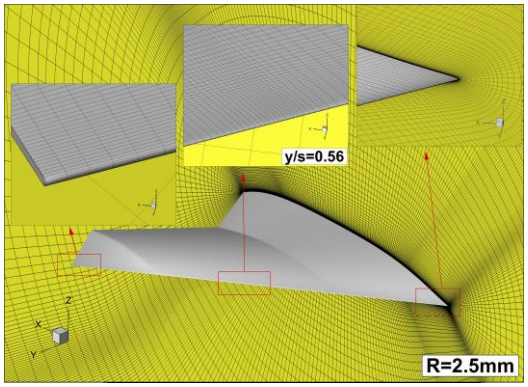

Figure 11: Cobalt near body grid distribution representations with leading edge topology zoom

[28] **U**nited **S**tates **A**ir **F**orce **R**esearch **L**aboratory
[29] **C**ourant-**F**riedrichs-**L**ewy
[30] **S**palart-**A**llmaras with **R**otational **C**orrection

3.3 Aerodynamic Design Studies

The following section presents the design study approaches and the effects on the flow topology of the MULDICON configuration, as well as on the aerodynamic performance and S&C behavior. For the latter one only the pitching moment characteristic is discussed. For an overall design to achieve an optimum in aerodynamic performance for the entire flight envelope an inverse design is appropriate, as long as attached flow is considered. The objectives of the current investigations are the influence of the vortical flow which could occur at medium to high angles of attack and the influence of design changes with respect to flow topology, aerodynamic performance and pitching moment characteristic. Thus, by taking the design constrains into account, the results and knowledge gained could later be applied to an inverse design to extend the range of the flight envelope of the aircraft. Even though the most critical flight points for MULDICON might be at a Mach number of 0.8, the studies presented in this section have all been performed at a Mach number of 0.4. This flow speed was selected as a compromise in order to avoid transonic effects in these fundamental studies, while still being compressible (making the process more stable). Following the conclusions from these first studies, a second step would then have to incorporate the transonic effects at a Mach number of 0.8, as well.

3.3.1 Airfoil Studies

This section discusses the influence of a variation of airfoils applied at location *A*, *B* and *C* (see Figure 7). The results of the numerical simulations using TAU is shown in Figure 12. Depicted are the lift (C_L), drag (C_D) and pitching moment (C_m) coefficient versus AoA[31] for four different airfoils. The Baseline configuration uses the SACCON airfoils (having varying radii over the wingspan) applied to the MULDICON planform. The other three are a typical supercritical airfoil, a symmetric NACA[32]-64A-010 and a cambered NACA-65A-410 airfoil. Besides the Baseline, the airfoils are adapted with the CST approach to apply a constant leading edge curvature radius of r = 1 mm related to a 1 m chord length (approx. 10 mm at full scale). The aim of the current design investigations is to provide a less complex topology in comparison to the SACCON leading edge contour distribution and to get rid of the discontinuity in the pitching moment which occurs for the SACCON at higher AoA, as described amongst others by Schütte et al. in [29].

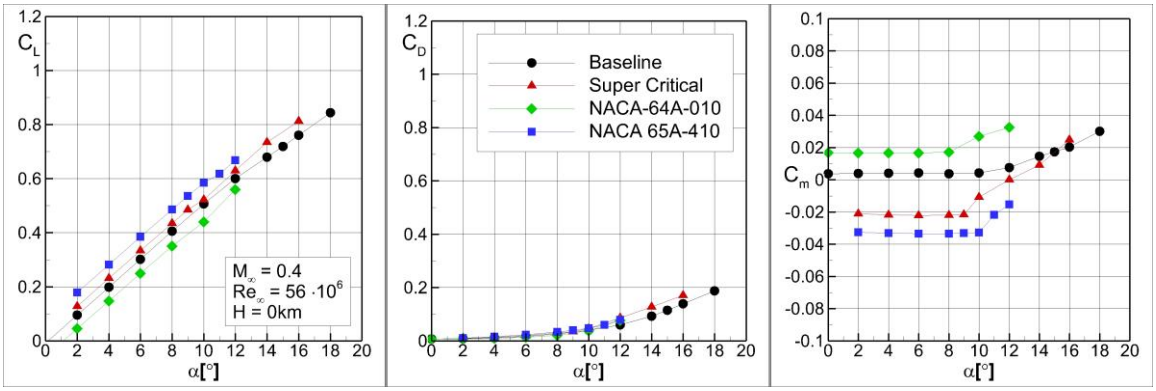

Figure 12: Lift, drag, and pitching moment coefficient versus AoA for MULDICON with different airfoils; TAU

The lift distribution versus AoA shows a quite similar linear behavior for all airfoils. The differences in lift versus AoA are based on a different cambering. The non-cambered NACA-65A-010 airfoil provides the lowest lift coefficient followed by the Baseline configuration, the Super Critical and the NACA-65A-410 airfoil. The same statement applies to the drag distribution. The pitching moment coefficient shows a neutral stability behavior ($C_m \approx$ const.) between 0° and 8° AoA for all applied airfoils. Due to the different cambering a significant difference in rear loading behavior occurs. For the Baseline the pitching moment coefficient is around 0, whereas the Super Critical and NACA-64A-410 airfoils provide negative values and the symmetric NACA airfoil provides positive ones. Beyond α = 10° an increase towards a more front loading pitching moment can be noted for all configurations.

The reason for this is the development of a leading edge vortex. While the flow is fully attached over the entire upper side of the wing for an angle of attack of α = 8°, the flow topology has completely changed for α = 12°. For all configurations besides the Baseline, a strong leading edge vortex has developed. These leading edge vortices provide a higher suction in front of the moment reference point in comparison to the suction behind it. For AoA higher than α = 12° this trend does not change because the starting point of the vortex at the leading edge moves towards the apex with increasing AoA. This vortex development behavior for swept wings with round leading edges has been already described by Schütte in [30] (see Figure 13) and should be one of the elements for the further design studies in the present article.

[31] **A**ngle **o**f **A**ttack
[32] **N**ational **A**dvisory **C**ommittee for **A**eronautics

The results for the Baseline configuration are presented to show the effect of the design changes in comparison to the SACCON configuration. In contrast to the first three configurations the leading edge contour distribution for SACCON is not constant along the span. The SACCON configuration has a sharp leading edge at the apex and wing tip which leads to a two-vortex-topology at an AoA of $\alpha = 12°$. Thus, the gradient of the pitching moment is less than for the configurations with only one vortex close to the apex. In comparison to the constant 10 mm radius for the other configurations the apex vortex is smaller due to a higher leading edge contour radius at section *B*. In addition to this the tip vortex compensates the nose up loading trend slightly.

More important is to note, that the pitching moment behavior is primarily defined by the leading edge contour. The reason for this effect is that the vortex occurrence, its progression and strength depend on the leading edge contour and not on the airfoil geometry. According to Figure 12, the increase in pitching moment occurs approximately at the same AoA.

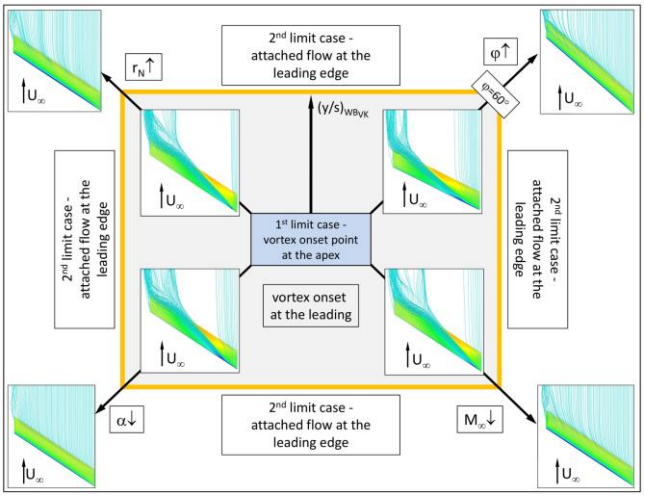

Figure 13: Overview of the assessed design rules: Effect of angle of attack, sweep angle, leading edge contour radius and Mach number (taken from [30])

3.3.2 Leading Edge Contour Studies

Referring to the results in the previous section the question arises how to influence the flow topology over the wing in a way such that the vortex development leads to a stable (or at least less unstable) pitching moment characteristic. This question leads to the second parametric study on the MULDICON planform dealing with the effect of the leading edge radius regarding the vortex development and related effects on the pitching moment characteristic. The first part of these investigations has been performed using the RANS solver Cobalt and the second part with the RANS solver DLR-TAU. Both, constant and linearly varying radii cases were simulated. Based on the design studies by Schütte [30], five different constant leading edge radii profiles were chosen, varying from 2.5 to 20 mm. Two varying leading edge profiles, linearly decreasing from apex to tip, were also chosen for investigation based on the results achieved in the constant leading edge radii profiles. Upon completion of these studies it should be possible to determine the relationship between leading edge radii and the overall aerodynamic characteristics of the MULDICON geometry. The leading edge contour radius distribution applied to the MULDICON is depicted in Figure 14.

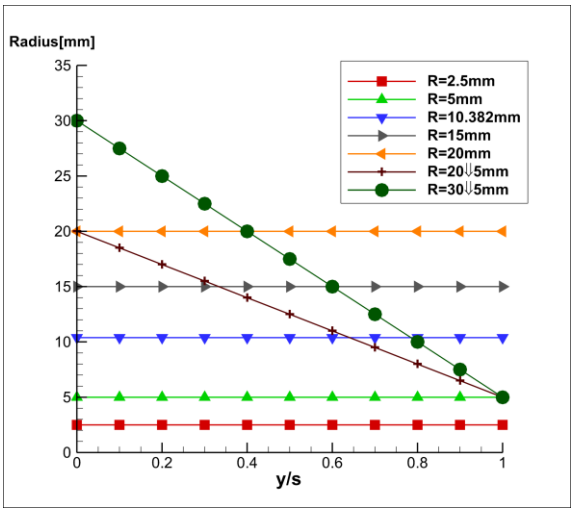

Figure 14: Leading edge contour radius distribution applied to MULDICON; Cobalt

Six different airfoils were provided for each airfoil section (*A*, *B* and *C*) along the MULDICON body by manipulating the leading edge contour radius. The predicted lift, drag and pitching moment coefficients for the various constant leading edge radius simulations are plotted against angle of attack in Figure 15. The Baseline MULDICON results are also plotted, providing a reference for evaluating the force characteristics of the modified geometries. A shift in lift coefficient occurs for all constant radius simulations, as seen in Figure 15. This increase in overall lift at a given AoA is due to the change in wing profiles as the NACA-65A-410 has more camber than the baseline MULDICON profiles. An increase in camber moves the angle of zero lift to more negative values, resulting in an upward shift in overall lift force for a given AoA.

All drag force coefficient data follows the same trend. However, with decreasing leading edge radius the drag force at medium to high angles of attack ($\alpha > 10°$) increases. For most streamline bodies a large portion of drag is related to skin friction, caused by the friction of the fluid passing over the body. The reason why drag often increases with angle of attack (aside from increasing induced drag) is an effect of flow separation creating larger amounts of pressure drag. The small radius cases tend to have higher amounts of drag, possibly related to earlier separation at low angles of attack. With larger radii profiles ($R \geq 10.382$ mm) the drag force is reduced at higher AoA. For $R = 30$ mm drag from $\alpha = 16°$ to $\alpha = 18°$ is consistently lower than for the Baseline case. The mid-range radii sizes, $R = 10 – 20$ mm, perform almost identical to that of the baseline data, with slight variation at $\alpha > 12°$.

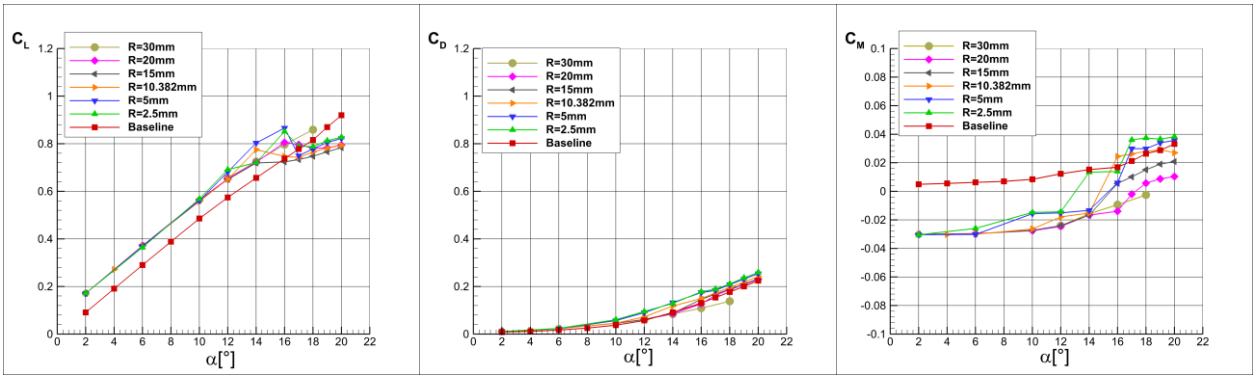

Figure 15: Lift, drag and pitching moment coefficient versus AoA for the various constant leading edge radius simulations; Cobalt

The predicted pitching moment coefficients for all constant radius cases have been shifted downward into the negative pitch regime at low angles of attack. All cases predict the same initial pitching moment coefficient of $C_M \approx -0.03$, significantly lower than the Baseline result, which predicts a $C_M = 0.05$. The positive camber of the airfoils gives rise to this shift, as a large camber value causes initial negative pitching moment behavior. For all cases the pitching moment tends to increase with increasing angle of attack, resulting in a positive slope and unstable pitching moment behavior. Furthermore, it can be seen that the increase in pitching moment slope corresponds with the break from linear in the lift coefficient-vs-alpha data. For the small radius case the pitch slope increases rather quickly, while for larger radii profiles a more neutral behavior is seen over a wider AoA range, visible with the almost zero slope region from $\alpha = 2°$ to $\alpha = 12°$. Further improvement is visible when increasing the leading edge radius to $R = 30$ mm, as the slope appears to be almost constant up to $\alpha = 18°$.

This type of UCAV aircraft is inherently unstable, requiring aileron deflection to provide proper pitch correction. The key is to avoid sudden changes in pitching moment over short angle of attack ranges, as it is almost impossible for the ailerons to compensate for such dramatic changes. Taking this into consideration the use of a large constant leading edge profile provides quite good pitch behavior for this aircraft type, as does the baseline MULDICON. For cases with a leading edge radius less than $R = 20$ mm, the stability characteristics are quite poor, providing little advantage when compared to the other leading edge designs. Thus, force results suggest that the use of a large leading edge radius would significantly improve the overall pitching moment characteristics, with secondary improvement in lift coefficient results. This finding goes well in line with the classical way of using round leading edges for conventional subsonic aircraft in order to delay separation.

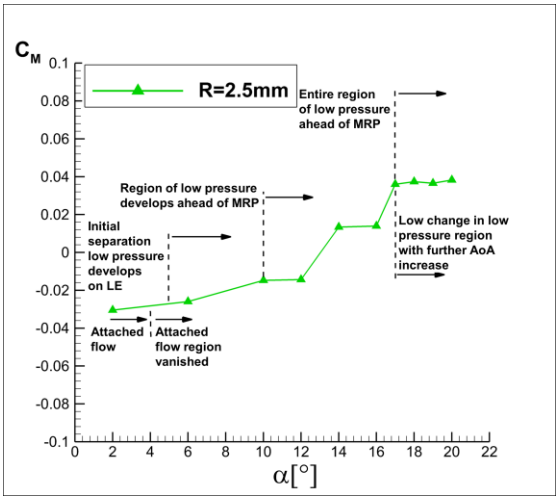

Figure 16: Effects of flow topology on the pitching moment for small constant leading edge radius geometry; Cobalt

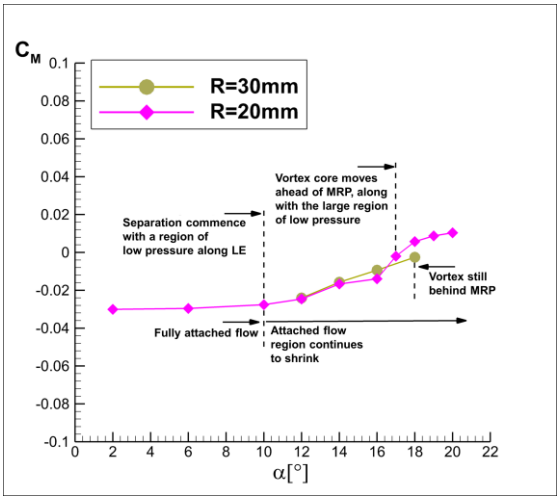

Figure 17: Effects of flow topology on the pitching moment for large constant leading edge radius geometries; Cobalt

Based on the findings discussed above, two diagrams were created in order to explain the effects of flow topology on the pitching moment characteristics for constant leading edge radius geometries. Figure 16 represents the lower limit of radii investigated ($R = 2.5$ mm), where unfavorable pitch behavior occurs. The second diagram, Figure 17, represents the upper limit of radii investigated ($R = 20 – 30$ mm), where a significant improvement in pitching moment performance over a wide angle of attack range is visible. Each of them will be discussed individually, in order to

describe the effects of the size of constant leading edge radius chosen.At low incidence angles, the case with R = 2.5 mm (Figure 16) exhibits fully attached flow with well distributed surface pressure over the upper surface of the MULDICON configuration. At $\alpha \approx 6°$ flow separation commences directly at the apex, spanning the entire leading edge, creating regions of low pressure which are well balanced relative to the MRP. Above $\alpha = 10°$, the separation behavior and resulting vortex roll-up strengthens, creating larger regions of low pressure that are not evenly distributed forward and aft of the MRP, which lead to an increase in pitching moment. From $\alpha = 10°$ to $\alpha = 12°$ these regions of low pressure across the entire leading edge re-balances, stalling any increase in pitching moment. This step like behavior in pressure distribution resulting in the destabilization of pitching moment repeats from $\alpha = 12°$ to $\alpha = 16°$. Above $\alpha = 16°$ a significant amount of the low pressure related to the vortex core has moved ahead of the MRP, resulting in a significant increase in pitching moment between $\alpha = 16°$ to $\alpha = 17°$. Above $\alpha = 17°$ the pitching moment behavior stays constant as the low pressure region ahead of the MRP does not strengthen by a substantial amount.

Deviation from this pitching moment behavior is significant with further increase in leading edge radii, as represented in Figure 17. At incidence angles below $\alpha = 10°$ the flow is fully attached, resulting in a neutral pitching moment characteristics (i.e. zero slope relative to *AoA*). At approximately $\alpha = 10°$ flow separation commences at the tip of the MULDICON planform, with a large region of low pressure across the entire leading edge. This low pressure region continues to strengthen with increasing angle of attack, while continually moving upstream towards the apex. Gradual increases in pitching moment occur as the region of low pressure behind the MRP continues to decrease in size, resulting in a pitch up characteristic as the distribution of pressure relative to the MRP is unbalanced. At an AoA just above $\alpha = 16°$ the vortex related to separation moves ahead of the MRP, resulting in a more significant rise in pitching moment. Above $\alpha = 17°$ the vortex continues to move upstream towards the apex, resulting in a steady increase in pitching moment. This rise in pitching moment is considerably more gradual in comparison to the smaller radius case. Variation is visible for the pitching moment characteristics of the largest radius case, R = 30 mm. As the upstream vortex movement is delayed with increase in angle of attack, also the rise in pitching moment is delayed to higher angles of incidence. The sudden increase in pitching moment is not visible below $\alpha = 18°$, a significant improvement in comparison to all other radii investigated. This is the reason, why the R = 30 mm case, together with a downward-twist of the wingtip to delay outboard separation, ("Case 8") was selected for the engine integration studies in the next section.

3.3.3 Engine Integration Studies

The purpose of this section is to provide the influence of the aerodynamic performance by integrating an engine intake and outlet and applying the related engine conditions. For these investigations, the configuration "Case 8" was selected from the parametric variations described above. It incorporates the NACA-65A-410 airfoils with R = 30 mm and a twist distribution of 0° for section *A*, -2° (around trailing edge) for section *B* and -3° (around leading edge) for section *C*. Figure 18 shows a comparison between the Case 8 clean configuration and the same configuration with a generic integrated engine intake and nozzle. It can be seen that the volume of the inner wing body section has not been increased but reduced between the engine inlet duct and the apex. The boundary conditions of the inlet and outlet surfaces as well as the engine conditions have been evaluated within a separate investigation from the Engine Integration Group. As described above, a Mach number of 0.4 has been chosen for the calculations with engine. The engine flight conditions chosen are the approach condition with a thrust level to provide a load factor of n_z = 2.5 estimating a mass of the aircraft of m = 13 000 kg.

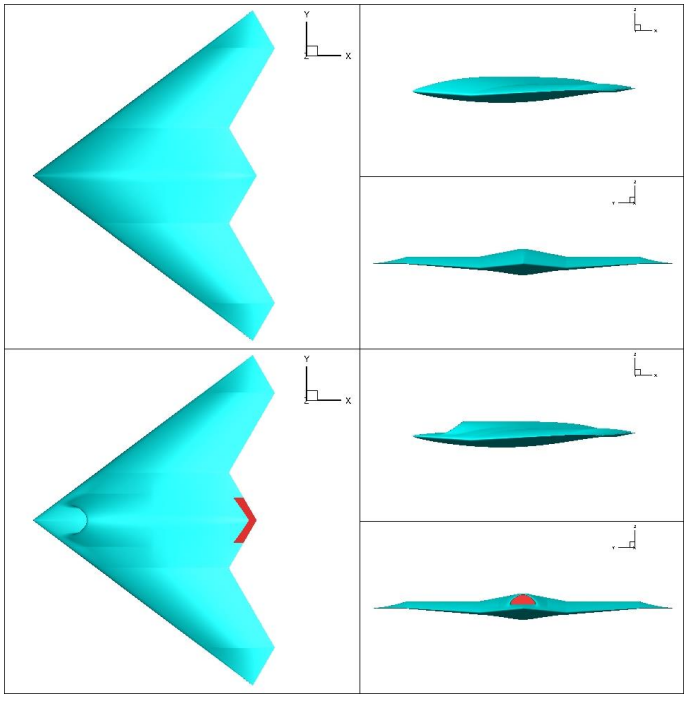

Figure 18: MULDICON design Case 8 (R = 30 mm) in clean configuration and with integrated engine inlet and outlet

Figure 19 shows a comparison of lift and pitching moment coefficients between the clean configuration and the configuration with integrated engine. The plots show that for the present investigation the lift and pitching moment are similar for the clean and the engine integrated configuration for the considered AoA range. The engine integration is neither affecting the longitudinal stability, nor the overall flow topology on the upper wing surface. Figure 20 shows the lift, drag, and thrust coefficients for the configuration with engine integration. In addition, the load factor is evaluated for AoA of 2° to 10°. For the present considered design point the load factor of n_z = 2.5 is provided at

an AoA of $\alpha = 6°$. The comparison between the drag versus thrust coefficient provides a slight lack of thrust of ≈ 80 drag counts. This is caused by the installation effects in comparison to the isolated engine evaluation and needs to be adjusted to receive a trimmed flight condition. Nevertheless, the present design matches the requirements quite well for the flight condition considered here.

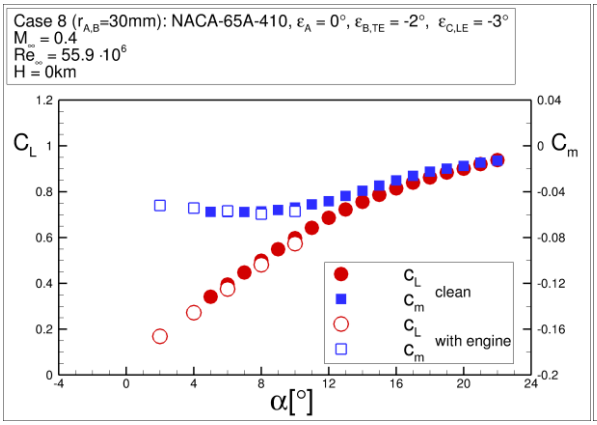

Figure 19: Lift and pitching moment versus AoA for Case 8 with and without engine integration; TAU

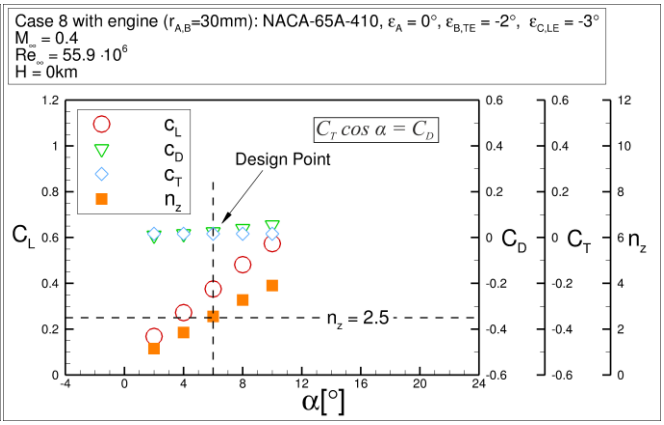

Figure 20: Lift, drag and thrust coefficient and load factor versus AoA for Case 8 with integrated engine; TAU

Figure 21 shows a comparison of the surface pressure distributions and flow topology on the upper surface of the clean MULDICON configuration at $\alpha = 6°$, as well as for the engine integration case for $\alpha = 6°$ and 10°. These plots show that the flow topology is not changed for the current flight condition (M = 0.4, Re = 55.9 million) with and without engine integration. Furthermore, it can be seen that the adjusted apex geometry for the configuration with engine meets the required regular onflow condition for the engine inlet. The inlet geometry does not cause flow disturbances ahead for the engine intake.

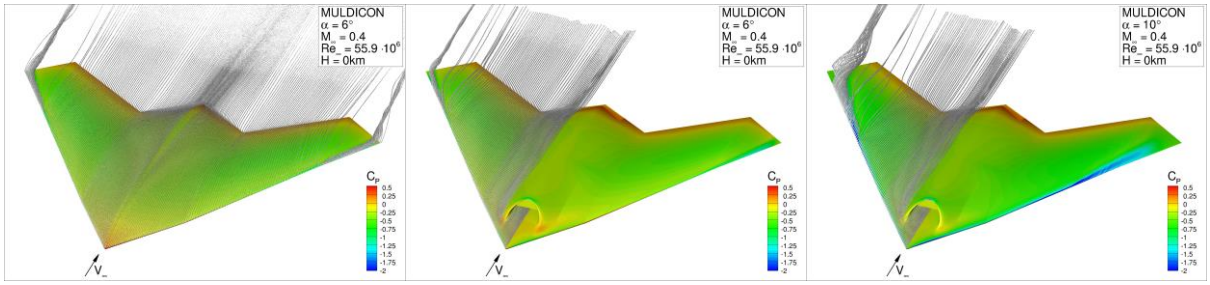

Figure 21: Flow topology on the upper wing with and without engine integration: Clean configuration at $\alpha = 6°$ (left), with engine at $\alpha = 6°$ (middle) and $\alpha = 10°$ (right); TAU

4 MULDICON Design

The overall aircraft design work for the MULDICON configuration was performed at DLR. It was based on the DLR conceptual design system, a flexible concept design toolset being developed since 2005 [44, 45]. This system consists of three components:

- A set of analysis tools representing the different disciplines of aircraft design.
- A flexible and extensible data exchange file format called CPACS[33], serving as common language for the analysis tools [46].
- The DLR integration framework software RCE[34], used for connecting the tools to build up task-specific analysis workflows [47].

Using this system, a process chain for investigating and assessing the MULDICON configuration was set up and applied. It contained the generation of aerodynamic and engine performance maps, a convergence loop for sizing important components of the aircraft, and a post-analysis for investigating performance and flying qualities of MULDICON. The whole process and the DLR design system itself are described in more detail by Liersch et al. in [48].

[33] **C**ommon **P**arametric **A**ircraft **C**onfiguration **S**chema
[34] **R**emote **C**omponent **E**nvironment

4.1 Results of the AVT-251 Design Teams

The design of the MULDICON configuration was a collaborative effort within the five design teams of AVT-251. This article focuses on the overall aircraft design aspects performed in the Design Specification and Assessment Group. However, the results from the other four teams are essential inputs to this work and are thus presented and discussed.

4.1.1 Aerodynamic Shaping

With respect to the outer shape, the Aerodynamic Shaping group provided a reference configuration first, which is identical to SACCON (same airfoils, same twist distribution), but with the modified trailing edge sweep of 30° (see section 3.1). In order to satisfy the requirements for maximum lift coefficient and pitching moment characteristics, two different design philosophies were applied to the reference configuration. The first one was focused on the understanding of the physical principles behind the complex vortex phenomena. Therefore, based on generic airfoils, parametric studies on varying leading edge radii and twist distributions were performed. Using these physical principles, the leading edge was shaped in a way that the movement of the vortices was minimized and the pitching moment curve became much smoother. An excerpt from these studies was presented in the previous chapter. More details on this approach are discussed by Schütte et al. in [49]. The second design approach aimed at minimizing vortex effects by designing for attached flow conditions. Therefore, a complete redesign of airfoil shapes and twist distribution was performed. Finally, the discontinuities in the pitching moment could be reduced and the maximum lift coefficient was increased. Details about this second, inverse design approach are given by Nangia et al. in [50]. Table 3 shows the achievements with respect to maximum lift coefficient. It can be seen that the design targets for these three points are nearly met. For the Combat High Altitude case the maximum lift coefficient is slightly lower than the design target, however, the lift demand for the 4.5 g maneuver is still reached.

Flight case	Load factor	Required lift coefficient	Target maximum lift coefficient	MULDICON	
				Baseline	Final Design
Takeoff	1.5	1.0	1.1	0.84 – 0.96	1.11 – 1.14
Combat High Altitude	4.5	0.717	0.817	0.61	0.72

Table 3: Maximum lift coefficients of MULDICON compared to requirements

For the conceptual design studies, all three versions (reference configuration and the two new designs) were modeled in the CPACS data format and investigated in the conceptual design workflow. At this point it turned out that the first design is not yet usable as its generic airfoils incorporate too much camber (causing a strong zero-lift pitch-down moment) for a flying wing aircraft. Since there were no resources available to apply the leading edge design to a more suitable set of airfoils, this concept was not investigated further. Thus, the second design concept, which is the official final design from the Aerodynamic Shaping group, is taken as main concept for the conceptual design studies (see Figure 22). The work of the Aerodynamic shaping Group as a whole is documented by van Rooij and Cummings in [51].

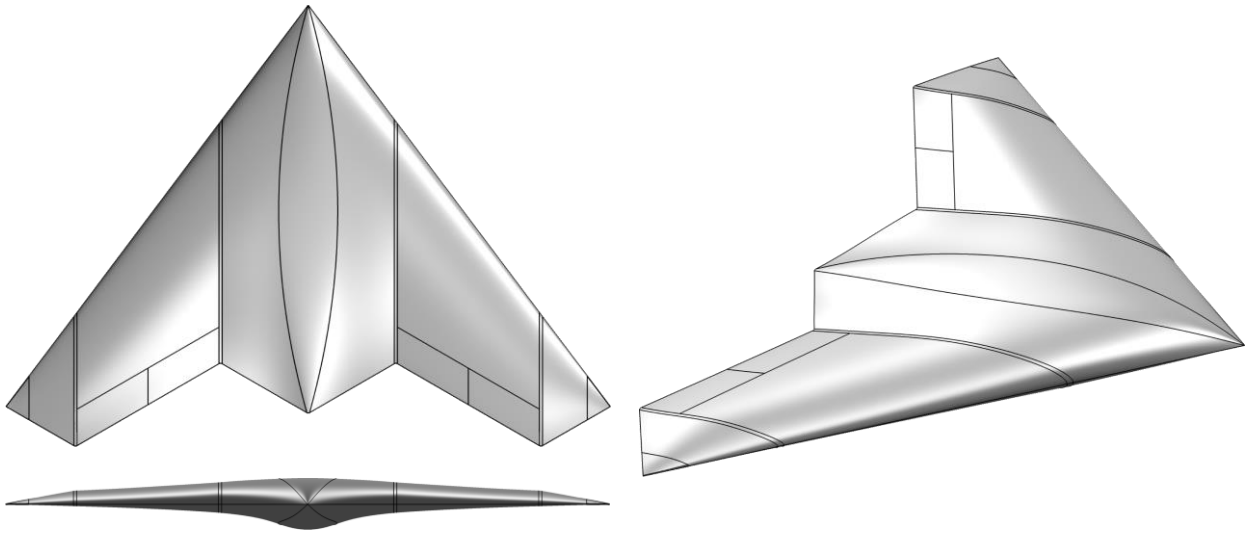

Figure 22: Outer shape of the MULDICON final configuration

4.1.2 Control Concept

The second main task in the development of MULDICON was the design of a suitable control concept, which is discussed by Löchert et al. in [28]. After confirming that the conventional trailing edge devices for roll and pitch

worked much better than they did for SACCON, the focus of this work was placed upon finding a solution for yaw control. As it was not clear at this point, how much yawing moment coefficient would be required, a target maximum value of 0.015 was chosen based on experience. In order to validate this value, an investigation with varying yaw control efficiency was performed by Hasan et al. [52] (Fig. 25, p. 27). Using the conceptual design workflow for simulating a landing maneuver with maximum permitted crosswind, it turned out that a yawing moment requirement of 0.015 seems to be reasonable for handling the permitted crosswind of 30 kn. The final control concept coming out of the Control Concept Group was applied to the MULDICON CPACS datasets.

4.1.3 Aerodynamic Shaping

Another important task was to provide an engine model which satisfies the engine design requirements, as specified in Chapter 2. This work was an additional contribution dedicated to AVT-251, in order to close a gap in the design capabilities of the group. Starting from a permitted fan diameter of 1 m, some engine design studies were performed. As it became clear, the fan diameter is still critical with respect to the integration of the engine and a corresponding intake and nozzle concept, a variation study for the fan diameter was performed. As a final result, a slightly smaller engine was selected and its performance tables were provided to the AVT-251 group. The engine design work and the sizing study are explained by Zenkner and Becker in [53]. The main engine parameters are provided in Table 4. With respect to engine integration into MULDICON, several studies were performed by the Engine Integration Group. Due to limitations in time and resources, their final results could not be incorporated directly into the overall aircraft concept. However, their demands were considered as boundary conditions where possible. More Details on engine integration work for MULDICON can be found in References [54-56].

Parameter	Condition	Unit	Value
Static thrust (dry)	*Takeoff*	*kN*	60
Bypass ratio	*Cruise*	–	1.7
Overall pressure ratio	*Takeoff*	–	30.5
Mass flow	*Takeoff*	*kg/s*	114
Turbine entry temperature	*Takeoff*	*K*	1 740
Specific fuel consumption	*Cruise*	*g/(kNs)*	23.8
Fan diameter	*all*	*m*	0.908
Length	*all*	*m*	2.2
Mass	*all*	*kg*	1 040

Table 4: Parameters of MULDICON engine "UCAV_G"

4.1.4 Structural Concept

The structural concept of MULDICON was defined by the Structural Concept Group. Based on experience and Finite Element analyses, the main structural elements were placed and sized, and an estimate for the structural mass of MULDICON was given. A special focus had to be placed on the big cutouts due to engine and payload/weapon bays and on aeroelastic effects like body-freedom-flutter. Further details about the structural and aeroelastic design work for MULDICON are presented in [57-60].

4.2 Overall Aircraft Design

Based on the results coming from the different design teams, the overall aircraft design work was performed at DLR. One of the central elements of the MULDICON workflow is a spreadsheet containing the main components of the aircraft and a two-dimensional planform view including the CG limits (see Figure 23). Using this spreadsheet, the main internal components were arranged. As can be seen in the diagram, large components e.g. engine were placed directly. Smaller components such as avionics boxes, for which the geometric properties are not known at this stage of the design cycle, were placed in free areas, assuming that they will have sufficient space there. The filled circles within the components shown represent the CG of that component. It was a difficult, iterative procedure to arrange all the components such that they have sufficient space, while the CG positions for all 11 weight & balance cases under investigation were kept within the specified limits between the red dashed lines. The CG range from the center of the aircraft is further displayed in a magnified detail sketch on the right side. The most forward location corresponds to the OEM[35] (no payload, no fuel) with landing gear up (GU), while the most rearward one represents the ferry flight case (no payload, maximum fuel) with landing gear down (GD). As an impression of the very tight limitations here, it shall be mentioned that for the operational empty mass case (yellow and green squares), the CG movement due to retracting the landing gear already uses around one third of the permitted CG range.

[35] **O**perational **E**mpty **M**ass case: aircraft ready to fly, but without fuel or payload

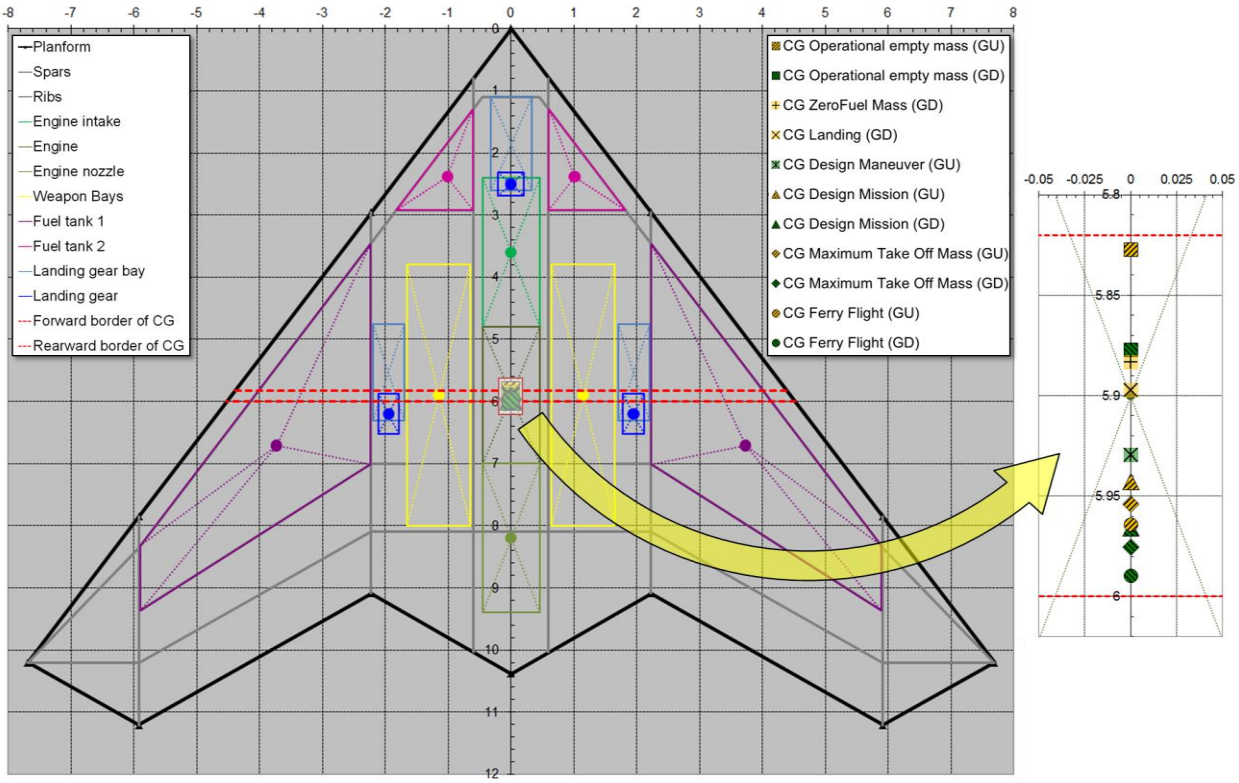

Figure 23: MULDICON planform with inner arrangement and CG locations

A mass breakdown of MULDICON, as calculated with the spreadsheet, is provided in Table 5. It contains the masses of the main components, their center of gravity locations and the mass moments of inertia for the main axis' around (0,0,0). The deviation moments are currently neglected, as well as the center of gravity locations in Z-direction (set to zero). Table 6 lists the selected weight and balance cases for MULDICON, together with the mass moments of inertia for the main axis' around the corresponding CG.

		CG Coordinates			Mass Moments of Inertia (0,0,0)		
Component	**Mass [*kg*]**	**X [*m*]**	**Y [*m*]**	**Z [*m*]**	**I_{xx} [*kgm²*]**	**I_{yy} [*kgm²*]**	**I_{zz} [*kgm²*]**
Structures	2 638	6.84	0.00	0.00	25 914	124 619	150 533
Landing gear (down)	321	5.29	0.00	0.00	920	9 796	10 716
Landing gear (up)	321	4.24	0.00	0.00	920	6 561	7 481
Propulsion	1 459	5.95	0.00	0.07	10	51 644	51 633
Systems	1 790	4.49	0.00	0.00	0	48 939	48 939
Other	559	5.93	0.00	0.00	595	19 673	20 268
OEM (GD)	**6 767**	**5.88**	**0.00**	**0.02**	**27 440**	**254 672**	**282 091**
OEM (GU)	**6 767**	**5.83**	**0.00**	**0.02**	**27 440**	**251 437**	**278 856**
Maximum payload	2 500	5.90	0.00	0.00	3 306	87 025	90 331
10% fuel (Landing)	367	6.11	0.00	0.00	8 288	26 081	34 368
66.7% fuel (Design Maneuver)	4 249	6.11	0.00	0.00	55 251	173 871	229 122
83.8% fuel (Design Mission)	5 341	6.11	0.00	0.00	69 441	218 524	287 964
100% fuel (MTOM, Ferry Flight)	6 374	6.11	0.00	0.00	82 877	260 806	343 683

Table 5: MULDICON component masses, CG locations, and mass moments of inertia around (0,0,0)

	Weight and balance case	Mass [*kg*]	CG Coordinates			Mass Moments of Inertia (CG)		
			X [*m*]	Y [*m*]	Z [*m*]	I_{xx} [kgm^2]	I_{yy} [kgm^2]	I_{zz} [kgm^2]
Gear Down	OEM	6 767	5.88	0.00	0.02	27 438	20 928	48 349
	ZFM[36]	9 267	5.88	0.00	0.01	30 745	20 929	51 656
	Landing[37]	7 404	5.90	0.00	0.01	35 726	23 250	58 959
	Design Mission[38]	14 607	5.97	0.00	0.01	100 186	40 299	140 467
	Ferry Flight[39]	13 141	5.99	0.00	0.01	110 316	44 017	154 314
	MTOM[40]	15 641	5.98	0.00	0.01	113 623	44 034	157 637
Gear Up	OEM	6 767	5.83	0.00	0.02	27 438	21 647	49 068
	Design Maneuver[41]	13 516	5.93	0.00	0.01	85 997	37 133	123 110
	Design Mission	14 607	5.94	0.00	0.01	100 186	41 088	141 255
	Ferry Flight	13 141	5.96	0.00	0.01	110 316	44 820	155 118
	MTOM	15 641	5.95	0.00	0.01	113 623	44 829	158 432

Table 6: MULDICON weight and balance cases, including mass moments of inertia around CG

One drawback of the spreadsheet is that it only contains a 2D model of the inner geometry, whereas the thickness of MULDICON varies continuously over the chord. As a consequence, from this model it is not possible to sufficiently determine, whether a component really fits into the outer shape. As a solution to this problem, the spreadsheet was extended by a so-called “Design Table” for Dassault's CATIA CAD software [61]. Combined with an existing CAD model of the MULDICON outer shape which also incorporates intake, nozzle and the control surfaces of the final control concept, the CATIA software uses the construction table to generate the inner components as specified in the spreadsheet. The CATIA 3D model of the UCAV configuration with its main components is shown in Figure 24.

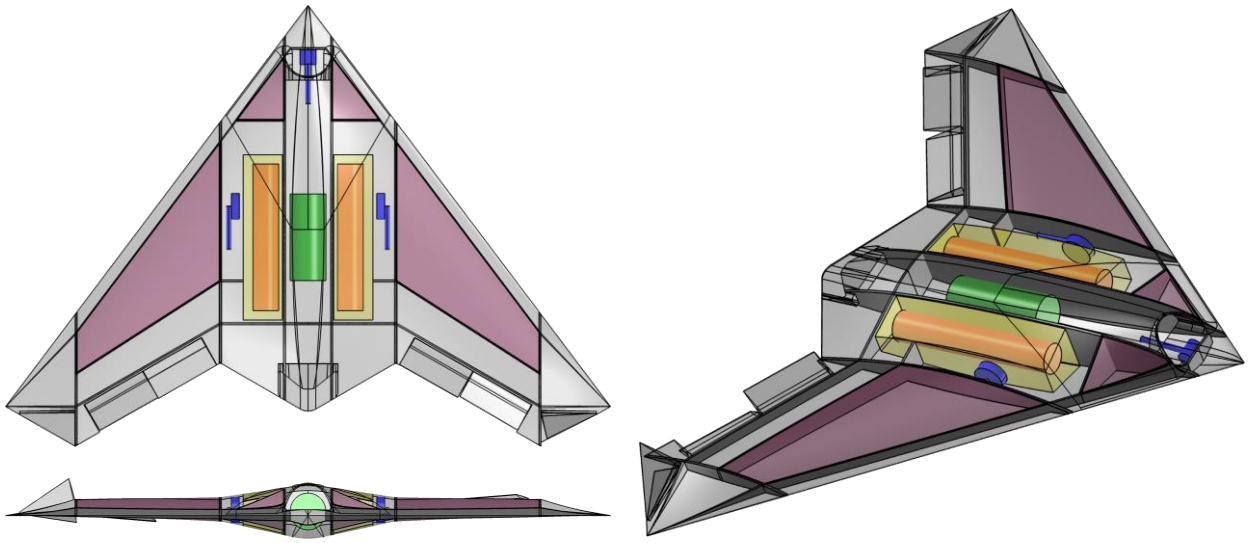

Figure 24: 3D model of MULDICON with internal arrangement

In the center of the convergence loop of the conceptual design process chain, the simulation of the design mission is located. After reaching convergence, the results for MULDICON final design show a required fuel mass of 5 341 kg and a flight duration of 3 hours and 18 minutes[42]. Compared to the maximum fuel capacity of 6 374 kg, the fuel reserve is 1 033 kg (or 16.2% of maximum fuel). With respect to an averaged mission fuel burn of 0.45 kg/s, this reserve would last for another 38 minutes of flight. Considering a fuel flow of around 0.17 kg/s, as it is present at the end of the cruise segment right before the final descent for landing, even a duration of 1 hour and 41 minutes is achieved. So, the design requirement of providing ≈ 45 minutes of fuel reserve after flying the design mission is satisfied. Compared to the

[36] **Z**ero **F**uel **M**ass case: OEM + maximum payload
[37] Landing case: OEM + landing fuel
[38] Design Mission case: OEM + mission fuel + maximum payload
[39] Ferry Flight case: OEM + maximum fuel
[40] MTOM case: OEM + maximum fuel + maximum payload
[41] Design Maneuver case: OEM + maneuver fuel + maximum payload
[42] It hast to be mentioned here that the mission simulation currently neglects the trim drag. However, with respect to the very small stability margin and the low zero-lift moment, the trim drag over the mission flight is assumed to be rather low.

MULDICON baseline configuration, the final design of MULDICON requires 304 kg (≈ 5.4%) less fuel for the design mission. In Figure 25, the main parameters of the aircraft are plotted over the flight time.

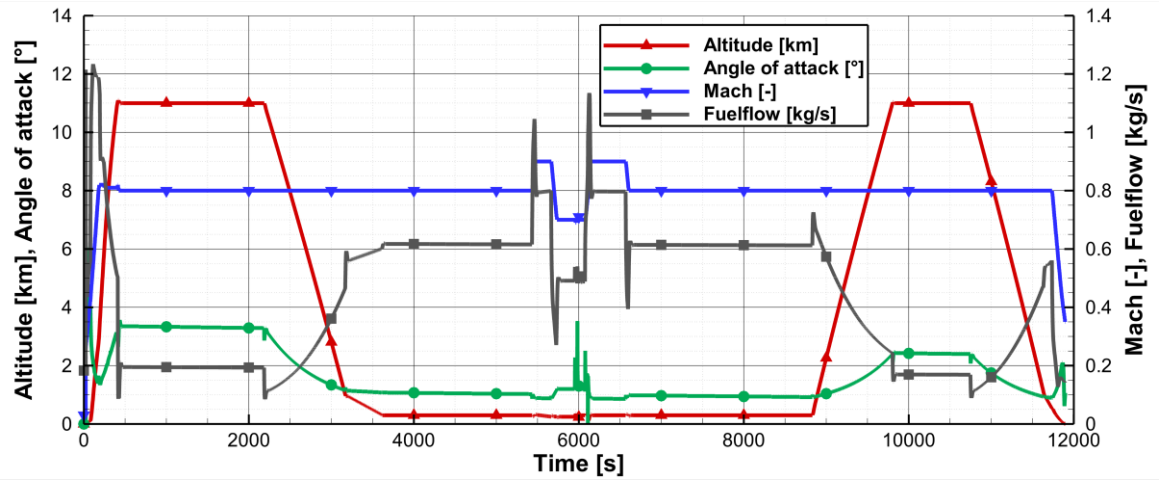

Figure 25: Trajectory of MULDICON, flying the design mission

After the end of the conceptual design workflow, a rather comprehensive CPACS dataset of the MULDICON configuration was made available, permitting further, more detailed investigations of the aircraft concept. One such investigation, which has not been published yet, was dedicated to flight performance and flying qualities evaluations. It shows that with respect to roll performance, the requirements for the "Takeoff" and "Combat High Altitude" cases could not be met sufficiently, while the other cases are within the specified limits. Furthermore, it turns out that the available thrust for the "Combat Low Altitude" case is not sufficient with respect to the sustained turn requirement – a consequence of a lift-to-drag assumption which turned out to be too optimistic for that case.

5 Summary

The foreground task of AVT-251 was to specify design requirements for an effective, agile UCAV, and then use these requirements to conduct a re-design of the SACCON configuration into a more realistic aircraft. In parallel, the background-task was to perform an assessment of how such a re-design could be performed within an AVT task group and how CFD could be effectively applied in such an early phase of the design process. Section 5.1 addresses the first question, while section 5.2 is dedicated to the second one. Finally, section 5.3 provides some conclusions drawn of the work being performed in AVT-251

5.1 Design Task

As a first step, a set of design requirements was put together and agreed on with the contributing partners of AVT-251. These requirements were selected to be typical for such sort of UCAV concepts, but highly ambitious with respect to the rather challenging SACCON configuration as a starting point. Due to the limited timeframe and resources it was not possible to work with a really comprehensive set of aircraft requirements. Instead, the demanded design targets were reduced to the most critical aspects and handed over to the various design teams. Next, a detailed design study took place with a number of aerodynamic shaping investigations. There were two distinct approaches that were followed by the Aerodynamic Shaping Group as they proceeded through the re-design: 1) design a new wing which was free of vortices during the mission. And 2) design a new wing which minimized the impact of the vortices on the aerodynamics of the vehicle. The enhancement of the SACCON concept had a number of specific goals, while still desiring to meet the mission requirements that had been applied to the original SACCON:

- Remove undesirable pitching moment characteristics
- Increase maximum lift coefficient
- Develop a control concept for sufficient roll, pitch, and yaw control
- Integrate an engine (intake & nozzle)
- Develop and size a structural concept, suitable for rigid and aeroelastic effects

After completing the various trade studies (including aerodynamic shaping and flow topology, structural layout and aeroelastics, as well as control concepts and flying qualities), a new configuration named MULDICON was found. The biggest change in the planform was the new trailing-edge sweep angle, which was greatly reduced compared to SACCON. It increased the internal volume, changed the CG locations, and made the control concepts more effective. A detailed engine installation study was also included as a last design detail, and while the engine inlets and outlets are still being improved, an acceptable design and internal layout was achieved for mission requirements and other

constraints. Reviewing the results from conceptual design and the different design teams, it has been demonstrated that the mission and payload requirements could be met. Regarding the agility requirements for the specified design points it can be summarized that there were not enough resources to investigate all five design points to the necessary extent and that one of the selected aerodynamic design paths could not be followed up to its end. However, for the addressed points the requirements could be satisfied or at least be nearly satisfied. The pitching moment characteristics for both MULDICON aerodynamic design paths have been smoothed – at least for the required range of lift coefficients. The new control concept fulfills most of its requirements, even though the roll performance for The "Takeoff" and "Combat High Altitude" cases is still insufficient; just as the thrust for doing a sustained 4.5 g turn under "Combat Low Altitude" conditions. With respect to this, coupling the results from the assessment back to the design teams and performing another design iteration would have been useful in order to fulfill the requirements completely. With regard to structures and aeroelasticity, a suitable solution for the structural concept has been found and investigated.

All of these design trade studies were carried out within the 3 year time period of AVT-251. While done without additional wind tunnel testing, the studies were performed with a high degree of confidence based on the large amount of wind tunnel data that was available for SACCON, making the CFD studies trustworthy within regular aircraft design accuracy levels.

5.2 Assessment Task

A detailed questionnaire was sent out to all participants of AVT-251 to obtain information about how well the task group operated, as well as basic information on time and computer hours that had been used to perform the work discussed in this paper. Finally the questionnaire has been filled out by 22 participants of the task group, which represents slightly over 50% of the members who participated in design groups. An effort was made to insure that key members of the design teams participated in the survey.

In order to put the assessment results in context, it is helpful to understand how the group operated. First of all, AVT-251 only met in person two times per year, which means the in-person meetings had to contain a great deal of time for the design teams to meet (approximately half of the meeting time was reserved for discipline team meetings). In order to make progress, many of the groups had to conduct tele-conferences at regular intervals between the in-person meetings in order to coordinate and update each other on group progress. All other communication for the design groups was conducted via email and phone calls among group members, as well as by using the group sharepoint site for exchanging documents and files. This situation represents an unusual situation for a typical aircraft design team, but in general the team managed to work together well and make reasonable progress.

Another important aspect which significantly contributes to the performance of the task group is the continuous recall of the aims and scientific problems to be answered by AVT-251, specifically:

- How do the tools contribute to the design process?
- How do the tools accelerate the design process?
- How do we arrange the tools in sequence or in parallel during the design process?
- To what degree CFD methods can provide sufficient data for a flight mechanics model?
- To what degree other disciplines can provide inputs to the process?

While focusing on the technical details and challenges of the MULDICON design work, these questions tended to be moved slightly into the background. Finally, the overall result of AVT-251 was definitely very positive, but it was challenging to keep everyone mindful of the full purpose of the task group. These are important considerations to keep in mind as the assessment results are looked at, but also if another task group with a similar purpose is proposed in the future.

First it is important to have a look at the time and computational resources expended to perform the overall design study. For the 22 participants who have filled out their questionnaire, a total of approximately 20 000 person-hours were used for participation in AVT-251. This includes attending task group meetings, participating in telecons, using the group sharepoint site, and other communication for the group, but also includes the total time spent performing the studies and analysis required for the design of MULDICON. Of the total hours spent, approximately 25% was spent within the DSAG (Design Specification and Assessment Group), 60% within the ASG (Aerodynamic Shaping Group), and 15% for all other groups (CCG, EIG, SCG). Within the ASG a total of 28.3 million CPU hours was used to perform the various CFD studies and analyses. Even though only half of the members answered the questionnaire, it can be stated that most of the key members of each design group (especially ASG where the vast majority of the CFD predictions were made) did contribute to the assessment survey, so the actual amount of CPU usage, for example, was probably not significantly higher than the 28.3 million hours reported above.

One aspect of the twice-yearly meetings was allowing significant time for each group to meet individually, and a few questions were asked about how those group meetings (and the groups themselves) functioned. On a scale of 1 to 10 (1 being extremely poor and 10 being excellent), the average response to how the group meeting format functioned yielded 7.33/10 with a standard deviation of 1.74. Considering the challenges of the logistics and space issues that took

place at our in-person meetings (where only one room was allotted for the total task group, hence breaking into 5 or 6 sub-groups required some groups meeting in hotel lobbies, etc.), this result was quite satisfactory. As for how well the groups functioned overall, the average was 7.50/10 with a standard deviation of 1.62. Again, this was a very satisfactory result and showed that, overall, the members of AVT-251 found the methods of meeting and communicating fairly successful.

The final questions of importance dealt with how well the overall design of MULDICON took place. The first question was "What is your impression of the overall collaboration effectiveness on the design of MULDICON (entire design across the group borders)." The response to this question was 6.40/10 with a standard deviation of 1.85. The final question was "Do you think the final MULDICON is a reasonable design for the requirements?" which had a response of 6.53/10 with a standard deviation of 1.50. While these results were slightly lower than the previous questions regarding how the sub-groups operated, they still represent reasonably good results for a task group that was only meeting twice a year, using a sharepoint site to share results and decisions, and occasional telecons. During the final meeting of AVT-251, several members mentioned that the typical constraints of an aircraft design process led to a great deal of work taking place in the final year of the task group, which did not allow for a re-evaluation and re-design to take place (as would normally be done in industry). Overall, AVT-251 operated quite well and the results were interesting and satisfactory for a team that met for a total of three years with the constraints discussed previously.

5.3 Conclusions

AVT-251 was a natural follow-on task group to AVT-161 and AVT-201.While these two groups had concentrated on the aerodynamics of the SACCON configuration, AVT-251 had taken on the challenge of making the vehicle able to achieve specific mission requirements that were typical for an advanced, agile UCAV configuration. The design trade studies were conducted within the framework of multiple teams, including design, aerodynamics, controls, structures, and engine integration. These teams were able to re-design SACCON with respect to certain constraints and requirements and came up with an enhanced configuration named MULDICON, which already satisfies most of these requirements. All of these studies and design aspects were conducted within a group that lasted for three years, while only meeting in person twice a year. The details of the design studies were included in four special sessions at the AIAA Aviation 2018 conference held in June 2018, followed by a special issue of the journal *Aerospace Science and Technology*, to which this article belongs. They are further published in the final report of AVT-251, which is currently in the publication process. The time and resource requirements of the study were recorded, as well as results of how well the task group worked and how effective the resulting design was able to achieve the requirements and constraints of the mission.

The major novelty of the AVT-251 design process is the fact that all the design work being performed was solely based on CFD simulations. During the extensive studies of the predecessor task groups, a great amount of experience on the shape of the developing flow structures, as well as on the correct application of modern CFD methods for such type of flow had been developed. Relying on this expertise and the corresponding confidence in the numerical results, the team members could perform a huge amount of different parameter studies in parallel – without the necessity to validate each single step by wind tunnel experiments. Even though this advantage cannot be quantified due to a lack of data for a comparable reference effort, it becomes obvious that a similar process incorporating extensive low- and high speed wind tunnel campaigns for a step-by-step evolving aircraft configuration (including control surface design and intake optimization) would not have been possible within a similar three-year task group.

So, this study represents a good example of how modern, well validated design and analysis tools can streamline the design process, as well as being able to come up with an enhanced configuration within a reasonable short period of time. The MULDICON configuration has similarities to a number of other modern UCAVs, and represents an already mostly satisfactory design that would have controllable flight characteristics at angles of attack that will make the configuration agile and capable of fulfilling more challenging missions.

6 Acknowledgments

The authors would like to acknowledge all of the nations, organizations, and individuals that participated in the various phases of the task group. Without the hard work and dedication of all of these contributors the work of the group would not have been possible.

The authors from DLR would like to thank the German MoD and The Federal Office of Bundeswehr Equipment, Information Technology and In-Service Support (BAAINBw) for their support for the military research at DLR and the support to attend the NATO STO/AVT Task Group meetings.

Russell Cummings would like to thank all of the members of the Task Groups that preceded and informed AVT-251, including AVT-113, AVT-161, AVT-183, and AVT-201. The hard work and dedication of the members of those task groups have made the work of AVT-251 possible.

The authors from UNB would like to thank the USAFA (Andrew Lofthouse and Matthew Satchell) for providing access to HPC clusters necessary to conduct the research.

7 References

[1] McDaniel, D., Cummings, R., Bergeron, K., Morton, S., and Dean, J., "Comparisons of CFD Solutions of Static and Maneuvering Fighter Aircraft with Flight Test Data," *3rd International Symposium on Integrating CFD and Experiments in Aerodynamics*, 2007, p. 39.

[2] Meyn, L. A., and James, K. D., "Full-scale wind-tunnel studies of F/A-18 tail buffet," *Journal of Aircraft*, Vol. 33, No. 3, 1996, pp. 589–595. doi: 10.2514/3.46986.

[3] Lovell, D. A., "Military Vortices," *NATO RTO / AVT Symposium on Advanced Flow Management*, Vol. RTO-MP-069-I, 2003.

[4] Jacobson, S., Britt, R., Freim, D., and Kelly, P., "Residual pitch oscillation (RPO) flight test and analysis on the B-2 bomber," *Structures, Structural Dynamics, and Materials and Co-located Conferences*, AIAA Paper 1998-1805, American Institute of Aeronautics and Astronautics, 1998. doi: 10.2514/6.1998-1805.

[5] Hall, R., Biedron, R., Ball, D., Bogue, D., Chung, J., Green, B., Grismer, M., Brooks, G., and Chambers, J., "Computational Methods for Stability and Control (COMSAC): The Time Has Come," *Guidance, Navigation, and Control and Co-located Conferences*, AIAA Paper 2005-6121, American Institute of Aeronautics and Astronautics, 2005. doi: 10.2514/6.2005-6121.

[6] "Vortex Breakdown over Slender Delta Wings," Final Report of the AVT-080 Task Group RTO-TR-AVT-080 AC/323(AVT-080)TP/253, NATO RTO / AVT, October 2009. doi: 10.14339/RTO-TR-AVT-080.

[7] Hummel, D., et al., "Understanding and Modeling Vortical Flows to Improve the Technology Readiness Level for Military Aircraft," Final Report of the AVT-113 Task Group RTO-TR-AVT-113 AC/323(AVT-080)TP/253, NATO RTO / AVT, October 2009. doi: 10.14339/RTO-TR-AVT-113.

[8] Hummel, D., "Review of the Second International Vortex Flow Experiment (VFE-2)," *Aerospace Sciences Meetings*, AIAA Paper 2008-377, American Institute of Aeronautics and Astronautics, 2008. doi: 10.2514/6.2008-377.

[9] Cummings, R. M., and Schütte, A., "Integrated Computational/Experimental Approach to Unmanned Combat Air Vehicle Stability and Control Estimation," *Journal of Aircraft*, Vol. 49, No. 6, 2012, pp. 1542–1557.

[10] Cummings, R. M., and Schütte, A., "Assessment of Stability and Control Prediction Methods for NATO Air and Sea Vehicles," Final Report of the AVT-161 Task Group RTO-TR-AVT-161 AC/323(AVT-161)TP/440, NATO RTO / AVT, September 2012. doi: 10.14339/RTO-TR-AVT-161.

[11] Hövelmann, A., and Breitsamter, C., "Leading-Edge Geometry Effects on the Vortex Formation of a Diamond-Wing Configuration," *Journal of Aircraft*, Vol. 52, No. 5, 2015, pp. 1596–1610. doi: 10.2514/1.C033014.

[12] Frink, N. T., "Numerical Analysis of Incipient Separation on 53-Deg Swept Diamond Wing," *AIAA SciTech Forum*, AIAA Paper 2015-88, American Institute of Aeronautics and Astronautics, 2015. doi: 10.2514/6.2015-0288.

[13] Cummings, R. M., Liersch, C. M., Schütte, A., and Huber, K. C., "Aerodynamics and Conceptual Design Studies on an Unmanned Combat Aerial Vehicle Configuration," *Journal of Aircraft*, Vol. 55, No. 2, 2018, pp. 454–474. doi: 10.2514/1.C033808.

[14] Cummings, R. M., and Schütte, A., "Extended Assessment of Stability and Control Prediction Methods for NATO Air Vehicles," Final Report of the AVT-201 Task Group STO-TR-AVT-201, NATO STO / AVT, November 2016. doi: 10.14339/STO-TR-AVT-201.

[15] Vicroy, D. D., Huber, K. C., Schütte, A., Rein, M., Irving, J. P., Rigby, G., Löser, T., Hübner, A.-R., and Birch, T. J., "Experimental Investigations of a Generic Swept Unmanned Combat Air Vehicle with Controls," *Journal of Aircraft*, Vol. 55, No. 2, 2016, pp. 475–501. doi: 10.2514/1.C033782.

[16] Huber, K. C., Vicroy, D. D., Schütte, A., and Hübner, A. R., "UCAV model design and static experimental investigations to estimate control device effectiveness and S&C capabilities," *AIAA AVIATION Forum*, AIAA-Paper 2014-2002, American Institute of Aeronautics and Astronautics, 2014. doi: 10.2514/6.2014-2002.

[17] Zimper, D., and Hummel, D., "Analysis of the Transonic Flow Around a Unmanned Combat Aerial Vehicle Configuration," *Journal of Aircraft*, Vol. 55, No. 2, 2016, pp. 571–586. doi: 10.2514/1.C033697.

[18] Coppin, J., Birch, T., Kennett, D., Hoholis, G., and Badcock, K., "Prediction of Control Effectiveness for a Highly Swept Unmanned Air Vehicle Configuration," *Journal of Aircraft*, Vol. 55, No. 2, 2016, pp. 534–548. doi: 10.2514/1.C033988.

[19] Ghoreyshi, M., Young, M. E., Lofthouse, A. J., Jirasek, A., and Cummings, R. M., "Numerical Simulation and Reduced-Order Aerodynamic Modeling of a Lambda Wing Configuration," *Journal of Aircraft*, Vol. 55, No. 2, 2016, pp. 549–570. doi: 10.2514/1.C033776.

[20] Schütte, A., Huber, K. C., Frink, N. T., and Boelens, O. J., "Stability and Control Investigations of Generic 53 Degree Swept Wing with Control Surfaces," *Journal of Aircraft*, Vol. 55, No. 2, 2016, pp. 502–533. doi: 10.2514/1.C033700.

[21] Cummings, R. M., Liersch, C. M., and Schütte, A., "Multi-Disciplinary Design and Performance Assessment of Effective, Agile NATO Air Vehicles," *AIAA AVIATION Forum*, American Institute of Aeronautics and Astronautics, 2018. doi: 10.2514/6.2018-2838.

[22] Liersch, C. M., Huber, K. C., Schütte, A., Zimper, D., and Siggel, M., "Multidisciplinary design and aerodynamic assessment of an agile and highly swept aircraft configuration," *CEAS Aeronautical Journal*, Vol. 7, No. 4, 2016, pp. 677–694. doi: 10.1007/s13272-016-0213-4.

[23] Department of Defense, USA, "GLOSSARY OF DEFINITIONS, GROUND RULES, AND MISSION PROFILES TO DEFINE AIR VEHICLE PERFORMANCE CAPABILITY," Military Standard, February 2003. MIL-STD-3013.

[24] Department of Defense, USA, "FLYING QUALITIES OF PILOTED AIRCRAFT," Military Standard, July 2001. MIL-STD-1797A.

[25] Liersch, C. M., and Huber, K. C., "Conceptual Design and Aerodynamic Analyses of a Generic UCAV Configuration," *AIAA AVIATION Forum*, American Institute of Aeronautics and Astronautics, 2014. doi: 10.2514/6.2014-2001.

[26] Schwithal, J., Rohlf, D., Looye, G., and Liersch, C. M., "An innovative route from wind tunnel experiments to flight dynamics analysis for a highly swept flying wing," *CEAS Aeronautical Journal*, Vol. 7, No. 4, 2016, pp. 645–662. doi: 10.1007/s13272-016-0214-3.

[27] Schütte, A., Huber, K. C., and Zimper, D., "Numerische aerodynamische Analyse und Bewertung einer agilen und hoch gepfeilten Flugzeugkonfiguration," *Deutscher Luft- und Raumfahrtkongress*, 2015.

[28] Löchert, P., Huber, K. C., Liersch, C. M., and Schütte, A., "Control Device Studies for Yaw Control without Vertical Tail Plane on a 53° Swept Flying Wing Configuration," *AIAA AVIATION Forum*, American Institute of Aeronautics and Astronautics, 2018. doi: 10.2514/6.2018-3329.

[29] Schütte, A., Hummel, D., and Hitzel, S. M., "Flow Physics Analyses of a Generic Unmanned Combat Aerial Vehicle Configuration," *Journal of Aircraft*, Vol. 49, No. 6, 2012, pp. 1638–1651. doi: 10.2514/1.C031386.

[30] Schütte, A., "Numerical Investigations of Vortical Flow on Swept Wings with Round Leading Edges," *Journal of Aircraft*, Vol. 54, No. 2, 2017, pp. 572–601. doi: 10.2514/1.C034057.

[31] Kroll, N., Langer, S., and Schwöppe, A., "The DLR Flow Solver TAU - Status and Recent Algorithmic Developments," *AIAA SciTech Forum*, AIAA Paper 2014-080, American Institute of Aeronautics and Astronautics, 2014. doi: 10.2514/6.2014-0080.

[32] Jameson, A., "Application of Dual Time Stepping to Fully Implicit Runge Kutta Schemes for Unsteady Flow Calculations," *AIAA AVIATION Forum*, AIAA Paper 2015-2753, American Institute of Aeronautics and Astronautics, 2015. doi: 10.2514/6.2015-2753.

[33] Spalart, P. R., and Allmaras, S. R., "A One-Equation Turbulence Model for Aerodynamic Flows," *Recherche Aerospatiale*, Vol. No. 1, 1994, pp. 5–21.

[34] Allmaras, S. R., Johnson, F. T., and Spalart, P. R., "Modifications and Clarifications for the Implementation of the Spalart-Allmaras Turbulence Model," *7th International Conference on Computational Fluid Dynamics, Big Island, Hawaii*, ICCFD7-1902, 2012.

[35] "CENTAUR Homepage," URL: http://www.centaursoft.com, [Accessed 15 February 2019].

[36] Strang, W., Tomaro, R., and Grismer, M., "The defining methods of Cobalt-60 - A parallel, implicit, unstructured Euler/Navier-Stokes flow solver," *Aerospace Sciences Meetings*, American Institute of Aeronautics and Astronautics, 1999. doi: 10.2514/6.1999-786.

[37] Gottlieb, J., and Groth, C., "Assessment of Riemann solvers for unsteady one-dimensional inviscid flows of perfect gases," *Journal of Computational Physics*, Vol. 78, 1988, pp. 437–458. doi: 10.1016/0021-9991(88)90059-9.

[38] Tomaro, R., Strang, W., Sankar, L., Tomaro, R., Strang, W., and Sankar, L., "An implicit algorithm for solving time dependent flows on unstructured grids," *Aerospace Sciences Meetings*, American Institute of Aeronautics and Astronautics, 1997. doi: 10.2514/6.1997-333.

[39] Tomaro, R. F., Strang, W. Z., and Wurtzler, K. E., "Can Legacy Codes Scale on Tens of Thousands of PEs or Do We Need to Reinvent the Wheel?" *High Performance Computing Modernization Program Contributions to DoD Mission Success*, DoD High Performance Computing Modernization Office, 2012, pp. 231–236.

[40] Lofthouse, A. J., Ghoreyshi, M., Jirasek, A., and Cummings, R. M., "Static and Dynamic Simulations of a Generic UCAV Geometry Using the Kestrel Flow Solver," *AIAA AVIATION Forum*, American Institute of Aeronautics and Astronautics, 2014. doi: 10.2514/6.2014-2264.

[41] "Cobalt User's Manual - Cobalt Version 6.0," Cobalt Solutions, LLC., February 2013.

[42] Kennett, D. J., Hoholis, G., and Badcock, K. J., "Numerical Simulation of Control Surface Deflections over a Generic UCAV configuration at Off-design Flow Conditions," *AIAA AVIATION Forum*, AIAA Paper 2014-2134, American Institute of Aeronautics and Astronautics, 2014. doi: 10.2514/6.2014-2134.

[43] Le Roy, J.-F., Morgand, S., and Farcy, D., "Static and Dynamic Derivatives on generic UCAV without and with leading edge control," *AIAA AVIATION Forum*, AIAA Paper 2014-2391, American Institute of Aeronautics and Astronautics, 2014. doi: 10.2514/6.2014-2391.

[44] Liersch, C. M., and Hepperle, M., "A distributed toolbox for multidisciplinary preliminary aircraft design," *CEAS Aeronautical Journal*, Vol. 2, No. 1-4, 2011, pp. 57–68. doi: 10.1007/s13272-011-0024-6.

[45] Nagel, B., Zill, T., Moerland, E., and Böhnke, D., "Virtual Aircraft Multidisciplinary Analysis and Design Processes - Lessons Learned from the Collaborative Design Project VAMP," *CEAS 2013 European Air and Space Conference*, 2013.

[46] Nagel, B., Böhnke, D., Gollnick, V., Schmollgruber, P., Rizzi, A., Rocca, G. L., and Alonso, J. J., "Communication in Aircraft Design: Can we establish a Common Language?" *28th International Congress of the Aeronautical Sciences (ICAS)*, 2012.

[47] Seider, D., Fischer, P., Litz, M., Schreiber, A., and Gerndt, A., "Open Source Software Framework for Applications in Aeronautics and Space," *IEEE Aerospace Conference*, 2012.

[48] Liersch, C. M., and Bishop, G., "Conceptual Design of a 53deg Swept Flying Wing UCAV Configuration," *AIAA AVIATION Forum*, American Institute of Aeronautics and Astronautics, 2018. doi: 10.2514/6.2018-2839.

[49] Schütte, A., Vormweg, J., Maye, R. G., and Jeans, T. L., "Aerodynamic shaping design and vortical flow design aspects of a 53deg swept flying wing configuration," *AIAA AVIATION Forum*, American Institute of Aeronautics and Astronautics, 2018. doi: 10.2514/6.2018-2841.

[50] Nangia, R. K., Coppin, J., and Ghoreyshi, M., "UCAV Wing Design, Assessment and Comparisons," *AIAA AVIATION Forum*, American Institute of Aeronautics and Astronautics, 2018. doi: 10.2514/6.2018-2842.

[51] van Rooij, M. P. C., and Cummings, R. M., "Aerodynamic design of an Unmanned Combat Air Vehicle in a collaborative framework," *AIAA AVIATION Forum*, American Institute of Aeronautics and Astronautics, 2018. doi: 10.2514/6.2018-2840.

[52] Hasan, Y. J., Flink, J., Freund, S., Klimmek, T., Kuchar, R., Liersch, C. M., Looye, G., Moerland, E., Pfeiffer, T., Schrader, M., and Zenkner, S., "Stability and Control Investigations in Early Stages of Aircraft Design," *AIAA AVIATION Forum*, American Institute of Aeronautics and Astronautics, 2018. doi: 10.2514/6.2018-2996.

[53] Zenkner, S., and Becker, R.-G., "Preliminary Engine Design for the MULDICON Configuration," *AIAA AVIATION Forum*, American Institute of Aeronautics and Astronautics, 2018. doi: 10.2514/6.2018-3163.

[54] Voß, C., Trost, M., and Becker, R.-G., "Automated Optimization of the MULDICON Inlet with Minimum Losses and Reduced Sight onto the Compressor Front Face," *AIAA AVIATION Forum*, American Institute of Aeronautics and Astronautics, 2018. doi: 10.2514/6.2018-3165.

[55] Edefur, H., Tormalm, M., Tysell, L., and Quas, M., "Design and Integration of a Low Observable Intake for the MULDICON Platform," *AIAA AVIATION Forum*, American Institute of Aeronautics and Astronautics, 2018. doi: 10.2514/6.2018-3162.

[56] Aref, P., Jirasek, A., Ghoreyshi, M., Cummings, R. M., and Satchell, M. J., "Computational Design of S-Duct Intakes for the NATO AVT-251 Multi-Disciplinary Configuration," *AIAA AVIATION Forum*, American Institute of Aeronautics and Astronautics, 2018. doi: 10.2514/6.2018-3164.

[57] Schweiger, J. M., Cunningham, A. M., Jr., Dalenbring, M., Voß, A., and Sakarya, E., "Structural Design Efforts for the MULDICON Configuration," *AIAA AVIATION Forum*, American Institute of Aeronautics and Astronautics, 2018. doi: 10.2514/6.2018-3325.

[58] Voß, A., "Gust Loads Calculation for a Flying Wing Configuration," *AIAA AVIATION Forum*, American Institute of Aeronautics and Astronautics, 2018. doi: 10.2514/6.2018-3326.

[59] Voß, G., Schaefer, D., and Vidy, C., "Investigations on flutter stability of the DLR-F19/SACCON configuration," *AIAA AVIATION Forum*, American Institute of Aeronautics and Astronautics, 2018. doi: 10.2514/6.2018-3327.

[60] Sakarya, E., Kocan, C., and Okumus, B., “A Study on Evaluation of Aeroelastic Characteristics of a UCAV Configuration,” *AIAA AVIATION Forum*, American Institute of Aeronautics and Astronautics, 2018. doi: 10.2514/6.2018-3328.

[61] “CATIA Homepage,” URL: http://www.3ds.com/de/produkte-und-services/catia/, [Accessed 15 February 2019].